

Inflationary magnetogenesis in the perturbative regime

Massimo Giovannini ¹

Department of Physics, CERN, 1211 Geneva 23, Switzerland

INFN, Section of Milan-Bicocca, 20126 Milan, Italy

Abstract

While during inflation a phase of increasing gauge coupling allows for a scale-invariant hyperelectric spectrum, when the coupling decreases a flat hypermagnetic spectrum can be generated for typical wavelengths larger than the effective horizon. After the gauge coupling flattens out the late-time hypermagnetic power spectra outside the horizon in the radiation epoch are determined by the hyperelectric fields at the end of inflation whereas the opposite is true in the case of decreasing coupling. Instead of imposing an abrupt freeze after inflation, we consider a smooth evolution of the mode functions by positing that the gauge couplings and their conformal time derivatives are always continuous together with the background extrinsic curvature. The amplified gauge power spectra are classified according to their transformation properties under the duality symmetry. After clarifying the role of the comoving and of the physical spectra in the formulation of the relevant magnetogenesis constraints, the parameter space of the scenario is scrutinized. It turns out that a slightly blue hyperelectric spectrum during inflation may lead to a quasi-flat hypermagnetic spectrum prior to matter radiation equality and before the relevant wavelengths reenter the effective horizon. In this framework the gauge coupling is always perturbative but the induced large-scale magnetic fields can be of the order of a few hundredths of a nG and over typical length scales between a fraction of the Mpc and 100 Mpc prior to the gravitational collapse of the protogalaxy.

¹e-mail address: massimo.giovannini@cern.ch

1 Introduction

Besides the invariance under local gauge transformations, the Weyl [1] and the duality [2, 3] symmetries are particularly relevant for the dynamics of the gauge fields in general relativity and in scalar-tensor theories of gravity. If the governing equations of a given field are invariant under Weyl rescaling, the corresponding quantum fluctuations are not parametrically amplified by the evolution of the geometry [4, 5, 6]. In the absence of sources duality rotates field strengths into their duals (i.e. tensors into pseudotensors) and constrains the gauge power spectra potentially amplified during conventional or unconventional inflationary phases.

The symmetries of the evolution equations of the gauge fields in curved space-times are one of the main handles on the origin of the large-scale magnetism, a perplexing problem originally posed by Fermi [7] in connection with the propagation of cosmic rays within the galaxy (see also [8]) and subsequently scrutinized by Hoyle [9] in a cosmological context in view of the comparatively large correlation scales of the fields. Indeed, while the typical diffusion scale in the interstellar medium is of the order of the AU ($1 \text{ AU} = 1.49 \times 10^{13} \text{ cm}$) magnetic fields are observed over larger scales ranging between the 30 kpc and few Mpc ($1 \text{ pc} = 3.08 \times 10^{18} \text{ cm}$).

Three general classes of suggestions have been proposed through the years. Soon after Hoyle's observations [9] Zeldovich [10] and of Thorne [11] suggested, in the context of anisotropic (but homogeneous) Bianchi-type models [12], that the large-scale magnetic fields could be a fossil remnant of a primordial field that originated with the Universe. In a complementary perspective we could imagine that the large-scale magnetic fields have been produced at some point during the radiation epoch and inside the Hubble radius by the vorticity associated with the turbulent dynamics; the first one suggesting this possibility was probably Harrison [13, 14] whose idea found direct applications in the context of phase transitions. Finally the third class of scenarios implies that a spectrum of gauge fields is produced because of the breaking of Weyl invariance during a standard stage of inflationary expansion; this is the perspective discussed in the present paper. The collection of themes related to the origin and to the early time effects of large-scale magnetism has been dubbed some time ago magnetogenesis [15]. While this terminology was so far quite successful, the problem itself has a long history as a number of inspiring monographs demonstrates [16, 17, 18]; see also Refs. [19, 20, 21] for some more recent reviews.

It has been repeatedly argued through the years that magnetic fields with a sufficiently large correlation scale could be generated during a phase of accelerated expansion in full analogy with what happens for the scalar and tensor modes of the geometry (see e.g. [22]). The gauge fields parametrically amplified in the early Universe are in fact divergenceless vector random fields that do not break the spatial isotropy (as it happens instead in the case of the fossil remnants discussed in Refs. [10, 11]). To avoid the constraints imposed by Weyl invariance the gauge fields might directly couple to one or more scalar fields (see [23, 24, 25, 26] for an incomplete list of references). The scalar fields may coincide with one or (more inflatons) or even with multiple spectator fields. This class of models is based on the following action:

$$S_{gauge} = -\frac{1}{16\pi} \int d^4x \sqrt{-G} \left[\lambda(\varphi, \psi) Y_{\alpha\beta} Y^{\alpha\beta} + \lambda_{pseudo}(\varphi, \psi) Y_{\alpha\beta} \widetilde{Y}^{\alpha\beta} \right]. \quad (1.1)$$

Within the present notations $Y^{\mu\nu}$ and $\widetilde{Y}^{\mu\nu}$ are, respectively, the gauge field strength and its dual; $G = \det G_{\mu\nu}$ is the determinant of the four-dimensional metric with signature mostly minus². In Eq. (1.1) φ denotes the inflaton field while ψ represents a generic spectator field. During a stage of conventional (slow-roll) inflation the variation of λ is associated with the variation of the gauge coupling whose evolution may reach into the strong coupling regime (see the third paper of Ref. [23]). The presence of $\lambda(\varphi, \psi)$ in Eq. (1.1) is more relevant than the pseudoscalar (axion-like [27, 28]) coupling which will be ignored even

²The Greek indices run over the four space-time dimensions while the Latin (lowercase) indices run over the three spatial dimensions. The signature of the four-dimensional metric will be mostly minus i.e. $(+, -, -, -)$. Finally the relation between the Riemann and the Ricci tensors will be chosen to be $R_{\mu\nu} = R^\alpha{}_{\mu\alpha\nu}$.

if it has been studied by many authors [29, 30, 31] in the context of the magnetic field generation. For the amplification of the magnetic field itself the pseudoscalar vertex is not essential but it may lead to hypermagnetic flux lines are linked or twisted as originally discussed in [32]. The produced Chern-Simons condensates leads to a viable (but unconventional) mechanism for baryogenesis via hypermagnetic knots [32, 33] which are characterized by an average magnetic gyrotropy [34]. These gyrotropic and helical fields play also a role in anomalous magnetohydrodynamics where the evolution of the magnetic fields at finite conductivity is analyzed in the presence of anomalous charges [35]. In the collisions of heavy ions this phenomenon is often dubbed chiral magnetic effect [36].

In this paper duality will be explicitly used to deduce the gauge power spectra not only during inflation but also during the subsequent decelerated expansion. We will show, in particular, that after the gauge coupling flattens out the late-time hypermagnetic power spectra outside the horizon in the radiation epoch are determined by the hyperelectric fields at the end of inflation whereas the opposite is true in the case of decreasing coupling. The obtained results suggest that a slightly blue hyperelectric spectrum during inflation may lead to a quasi-flat hypermagnetic spectrum prior to matter radiation equality and before the relevant wavelengths reenter the effective horizon. From the technical viewpoint these results will arise from the discussion of an appropriate transition matrix whose elements have well defined transformation properties under the duality symmetry and control the form of the late-time spectra. Using these results we shall investigate the magnetogenesis requirements as well as all other pertinent constraints; we shall conclude that large-scale magnetic fields can be generated during a quasi-de Sitter stage of expansion while the gauge coupling remains perturbative throughout all the stages of the dynamical evolution.

The layout of this paper is in short the following. In section 2 after introducing the necessary generalities, we shall discuss the duality symmetry both for the field equations and for the power spectra. At the end of the section we shall discuss two complementary (and dual) profiles for the evolution of the gauge couplings. In section 3 the gauge power spectra during inflation will be computed for typical wavelengths larger than the effective horizon and related via duality transformations. Using the overall continuity of the whole description the electric and the magnetic mode functions at the end of inflation will be explicitly related, in section 4, to the gauge spectra in the radiation epoch via a transition matrix whose elements transform in a well defined way under duality. The gauge spectra will then be computed in several approximations schemes with particular attention to the relevant phenomenological regimes. In section 5 the magnetogenesis requirements will be examined in conjunction with the physical constraints. Section 6 contains our concluding remarks. To avoid lengthy digressions various technical results have been relegated to the appendices A, B and C.

2 Equations of motion, duality and dynamical gauge couplings

With the purpose of making the whole discussion self-contained, the essential notations will be introduced in the first part of this section while in the second part we shall examine the gauge power spectra in the light of the duality symmetry. In the last part of the section the physical aspects of the evolution of the gauge couplings will be specifically addressed.

2.1 Notations, conventions and some general considerations

The field content of the model may be different but it generally follows from a total action of the type:

$$S_{tot} = S_{grav} + S_{scalar} + S_{gauge}, \quad (2.1)$$

where S_{gauge} has been already introduced in Eq. (1.1) and, as already mentioned, $Y_{\mu\nu}$ and $\widetilde{Y}^{\mu\nu}$ denote, respectively, the gauge field strength and its dual:

$$\widetilde{Y}^{\mu\nu} = \frac{1}{2} E^{\mu\nu\rho\sigma} Y_{\rho\sigma}, \quad E^{\mu\nu\rho\sigma} = \frac{\epsilon^{\mu\nu\rho\sigma}}{\sqrt{-G}}. \quad (2.2)$$

In Eq. (2.2) $\epsilon^{\mu\nu\rho\sigma}$ denotes the totally antisymmetric symbol of Levi-Civita in four dimensions. In more explicit terms the gravitational and the scalar actions of Eq. (2.1) can be expressed as:

$$\begin{aligned} S_{grav} &= -\frac{1}{2\ell_P^2} \int d^4x \sqrt{-G} R, \\ S_{scalar} &= \int d^4x \sqrt{-G} \left[\frac{1}{2} G^{\alpha\beta} \partial_\alpha \varphi \partial_\beta \varphi + \frac{1}{2} G^{\alpha\beta} \partial_\alpha \psi \partial_\beta \psi - W(\varphi, \psi) \right], \end{aligned} \quad (2.3)$$

where $\ell_P^2 = 1/\overline{M}_P^2 = 8\pi/M_P^2$ and $M_P = 1.22 \times 10^{19}$ GeV is the Planck mass. The notations of Eq. (2.3) are purposely schematic and φ denotes the inflaton while ψ is a spectator field. Various magnetogenesis models have been discussed in various contexts where $W(\varphi, \psi)$ has a well defined expression. For instance in the models of Ref. [23] W is only function of φ while an explicit magnetogenesis model based on spectator fields can be found in the last paper of Ref. [24]. With these specifications, the general equations derived from the actions (2.1)–(2.3) are:

$$R_\mu^\nu = \ell_P^2 \left[\partial_\mu \varphi \partial^\nu \varphi - W \delta_\mu^\nu + \mathcal{T}_\mu^\nu \right], \quad (2.4)$$

$$G^{\alpha\beta} \nabla_\alpha \nabla_\beta \varphi + \frac{\partial W}{\partial \varphi} + \frac{1}{16\pi} \frac{\partial \lambda}{\partial \varphi} Y_{\alpha\beta} Y^{\alpha\beta} = 0, \quad (2.5)$$

$$\nabla_\alpha \left(\lambda Y^{\alpha\beta} \right) = 0, \quad \nabla_\alpha \tilde{Y}^{\alpha\beta} = 0. \quad (2.6)$$

In Eq. (2.4) \mathcal{T}_μ^ν denotes the (traceless) energy-momentum tensor of the gauge fields whose explicit form is given by:

$$\mathcal{T}_\mu^\nu = \frac{\lambda}{4\pi} \left[-Y_{\mu\alpha} Y^{\nu\alpha} + \frac{1}{4} \delta_\mu^\nu Y_{\alpha\beta} Y^{\alpha\beta} \right]. \quad (2.7)$$

We shall be mostly concerned with conformally flat background geometries whose associated line element is:

$$ds^2 = G_{\alpha\beta} dx^\alpha dx^\beta = a^2(\tau) [d\tau^2 - d\vec{x}^2], \quad (2.8)$$

where $a(\tau)$ denotes the scale factor. In the geometry (2.8) the various components of \mathcal{T}_μ^ν defined in Eq. (2.7) are:

$$\begin{aligned} \mathcal{T}_0^0 &= \rho_B + \rho_E, & \mathcal{T}_0^i &= \frac{1}{4\pi a^4} (\vec{E} \times \vec{B})^i, \\ \mathcal{T}_i^j &= -(p_E + p_B) \delta_i^j + \Pi_{Ei}^j + \Pi_{Bi}^j. \end{aligned} \quad (2.9)$$

In Eq. (2.9) we introduced the energy density, the pressure and the anisotropic stresses of the hypermagnetic and hyperelectric fields:

$$\rho_B = \frac{B^2}{8\pi a^4}, \quad \rho_E = \frac{E^2}{8\pi a^4}, \quad p_B = \frac{\rho_B}{3}, \quad p_E = \frac{\rho_E}{3}, \quad (2.10)$$

$$\Pi_{Ei}^j = \frac{1}{4\pi a^4} \left(E_i E^j - \frac{E^2}{3} \delta_i^j \right), \quad \Pi_{Bi}^j = \frac{1}{4\pi a^4} \left(B_i B^j - \frac{B^2}{3} \delta_i^j \right), \quad (2.11)$$

where $E^2 = \vec{E} \cdot \vec{E}$ and $B^2 = \vec{B} \cdot \vec{B}$. Equations (2.9), (2.10) and (2.11) are expressed in terms of \vec{E} and \vec{B} , i.e. the *comoving* hyperelectric and hypermagnetic fields. These rescaled quantities are actually the normal modes of the system and are related to the *physical* fields as:

$$\vec{E} = a^2 \sqrt{\lambda} \vec{E}^{(phys)}, \quad \vec{B} = a^2 \sqrt{\lambda} \vec{B}^{(phys)}. \quad (2.12)$$

The components of the field strengths can be directly expressed in terms of the components of the physical fields; so for instance, in terms of ϵ^{ijk} (i.e. the Levi-Civita symbol in three dimensions) we have

$$Y_{i0} = -a^2 E_i^{(phys)}, \quad Y^{ij} = -\epsilon^{ijk} B_k^{(phys)} / a^2, \quad (2.13)$$

and similarly for the dual strength. The physical fields are essential for the discussion of the actual magnetogenesis constraints but the evolution equations of (2.6) are simpler in terms of the comoving fields:

$$\vec{\nabla} \cdot (\sqrt{\lambda} \vec{E}) = 0, \quad \vec{\nabla} \cdot \left(\frac{\vec{B}}{\sqrt{\lambda}} \right) = 0, \quad (2.14)$$

$$\partial_\tau (\sqrt{\lambda} \vec{E}) = \vec{\nabla} \times \left(\sqrt{\lambda} \vec{B} \right), \quad \partial_\tau \left(\frac{\vec{B}}{\sqrt{\lambda}} \right) = -\vec{\nabla} \times \left(\frac{\vec{E}}{\sqrt{\lambda}} \right). \quad (2.15)$$

Equations (2.14)–(2.15) have been written in the general case where λ can be inhomogeneous even if, as we shall see in the last part of this section, the gauge coupling will always be considered to be time-dependent but homogeneous. Furthermore Eqs. (2.14)–(2.15) under the following duality tranformation:

$$\sqrt{\lambda} \rightarrow \frac{1}{\sqrt{\lambda}}, \quad \vec{B} \rightarrow \vec{E}, \quad \vec{E} \rightarrow -\vec{B}. \quad (2.16)$$

All the mode functions and power spectra obtained by the simultaneous evolution of the geometry and of the gauge coupling must be consistent with Eq. (2.16) both during the inflationary phase and in the subsequent decelerated stages of expansion before the given scale reenters the effective horizon. The gauge coupling $e(\lambda)$ is related to the inverse of $\sqrt{\lambda}$:

$$S_{gauge} = -\frac{1}{4} \int d^4x \frac{\sqrt{-G}}{e^2} Y_{\mu\nu} Y^{\mu\nu}, \quad e^2 = \frac{4\pi}{\lambda}. \quad (2.17)$$

Thus the gauge coupling increases when λ decreases and vice versa.

2.2 Quantization and canonical form of the power spectra

Since we are going to discuss the parametric amplification of the quantum fluctuations of the gauge fields the classical evolution summarized by Eqs. (2.14)–(2.15) must be complemented by the corresponding quantum treatment. From the semi-classical viewpoint this process can be viewed as the conversion of traveling waves into standing waves; the same phenomenon occurs for the scalar and tensor modes of the geometry [22] and it leads to the so-called Sakharov oscillations [37] (see also [38, 39, 40]). In the present context the duality symmetry explicitly relates the Sakharov oscillations of the hypermagnetic [i.e. $f_{k,\alpha}(\tau)$] and hyperelectric mode functions [i.e. $g_{k,\alpha}(\tau)$] entering the expressions of the corresponding field operators:

$$\hat{B}_i(\tau, \vec{x}) = -\frac{i\epsilon_{mni}}{(2\pi)^{3/2}} \sum_{\alpha=\oplus, \otimes} \int d^3k k_m e_n^{(\alpha)}(\hat{k}) \left[f_{k,\alpha}(\tau) \hat{a}_{\vec{k},\alpha} e^{-i\vec{k}\cdot\vec{x}} - f_{k,\alpha}^*(\tau) \hat{a}_{\vec{k},\alpha}^\dagger e^{i\vec{k}\cdot\vec{x}} \right], \quad (2.18)$$

$$\hat{E}_i(\tau, \vec{x}) = -\frac{1}{(2\pi)^{3/2}} \sum_{\alpha=\oplus, \otimes} \int d^3k e_i^{(\alpha)}(\hat{k}) \left[g_{k,\alpha}(\tau) \hat{a}_{\vec{k},\alpha} e^{-i\vec{k}\cdot\vec{x}} + g_{k,\alpha}^*(\tau) \hat{a}_{\vec{k},\alpha}^\dagger e^{i\vec{k}\cdot\vec{x}} \right]. \quad (2.19)$$

In Eqs. (2.18)–(2.19) the two vector polarizations are directed along the orthogonal unit vectors \hat{e}_\oplus and \hat{e}_\otimes that are also orthogonal to \hat{k} (i.e. $\hat{k} \cdot \hat{e}_\alpha = 0$). In Eq. (2.19) $\hat{a}_{\vec{k},\alpha}$ and $\hat{a}_{\vec{k},\alpha}^\dagger$ are the creation and annihilation operators obeying, within the present notations, $[\hat{a}_{\vec{q},\alpha}, \hat{a}_{\vec{p},\beta}^\dagger] = \delta^{(3)}(\vec{q} - \vec{p}) \delta_{\alpha\beta}$. In Eqs. (2.18) and (2.19) the sum is performed over the physical polarizations $e_i^{(\alpha)}(\hat{k})$ while the mode functions $f_{k,\alpha}$ and $g_{k,\alpha}$ obey, in the absence of conductivity, the following pair of equations:

$$f'_{k,\alpha} = g_{k,\alpha} + \mathcal{F} f_{k,\alpha}, \quad g'_{k,\alpha} = -k^2 f_{k,\alpha} - \mathcal{F} g_{k,\alpha}, \quad \mathcal{F} = \frac{\sqrt{\lambda}'}{\sqrt{\lambda}}, \quad (2.20)$$

where the prime denotes a derivation with respect to the conformal time coordinate τ . The mode functions in Eq. (2.20) must also be correctly normalized so that the Wronskian of any solution must satisfy for each polarization:

$$f_{k,\alpha}(\tau) g_{k,\alpha}^*(\tau) - f_{k,\alpha}^*(\tau) g_{k,\alpha}(\tau) = i. \quad (2.21)$$

The field operators of Eqs. (2.18)–(2.19) can be represented in Fourier space as³

$$\begin{aligned} \hat{B}_j(\vec{p}, \tau) &= -i p_m \epsilon_{mnj} \sum_{\beta} \left[e_n^{\beta}(\hat{p}) \hat{a}_{\vec{p},\beta} f_{q,\beta}(\tau) + e_n^{\alpha}(-\hat{p}) \hat{a}_{-\vec{p},\beta}^{\dagger} f_{p,\beta}^*(\tau) \right], \\ \hat{E}_i(\vec{q}, \tau) &= \sum_{\alpha} \left[e_i^{\alpha}(\hat{q}) \hat{a}_{\vec{q},\alpha} g_{q,\alpha}(\tau) + e_i^{\alpha}(-\hat{q}) \hat{a}_{-\vec{q},\alpha}^{\dagger} g_{q,\alpha}^*(\tau) \right]. \end{aligned} \quad (2.22)$$

Therefore the corresponding two-point functions in Fourier space become:

$$\langle \hat{B}_i(\vec{k}, \tau) \hat{B}_j(\vec{p}, \tau) \rangle = \frac{2\pi^2}{k^3} P_B(k, \tau) p_{ij}(\hat{k}) \delta^{(3)}(\vec{k} + \vec{p}), \quad (2.23)$$

$$\langle \hat{E}_i(\vec{k}, \tau) \hat{E}_j(\vec{p}, \tau) \rangle = \frac{2\pi^2}{k^3} P_E(k, \tau) p_{ij}(\hat{k}) \delta^{(3)}(\vec{k} + \vec{p}), \quad (2.24)$$

where $p(\hat{k}) = (\delta_{ij} - \hat{k}_i \hat{k}_j)$; $P_B(k, \tau)$ and $P_E(k, \tau)$ are the *comoving magnetic and electric power spectra*, respectively⁴:

$$P_B(k, \tau) = \frac{k^5}{4\pi^2} \sum_{\alpha=\oplus, \otimes} |f_{k,\alpha}(\tau)|^2 \equiv \frac{k^5}{2\pi^2} |f_k(\tau)|^2, \quad (2.25)$$

$$P_E(k, \tau) = \frac{k^3}{4\pi^2} \sum_{\alpha=\oplus, \otimes} |g_{k,\alpha}(\tau)|^2 \equiv \frac{k^3}{2\pi^2} |g_k(\tau)|^2. \quad (2.26)$$

For the present purposes it will be important to distinguish the comoving from the physical power spectra: while the comoving power spectra are obtained from the comoving field operators \hat{B}_i and \hat{E}_i , the *physical power spectra* follow from the corresponding physical fields $\hat{E}_i^{(phys)}$ and $\hat{B}_i^{(phys)}$, defined in Eq. (2.12); the relation between the physical and the comoving power spectra is therefore given by:

$$P_B^{(phys)}(k, \tau) = \frac{P_B(k, \tau)}{\lambda(\tau)a^4(\tau)}, \quad P_E^{(phys)}(k, \tau) = \frac{P_E(k, \tau)}{\lambda(\tau)a^4(\tau)}. \quad (2.27)$$

The phenomenological requirements (e.g. the magnetogenesis constraints to be discussed in section 5) must be typically expressed in terms of the physical spectra. Occasionally this distinction has not been clearly spelled out and the consequences have been confusing, as we shall remark later on. Let us conclude this discussion by recalling that the two coupled first-order equations given in Eq. (2.20) can be transformed in two (decoupled) second-order differential equations:

$$f_{k,\alpha}'' + \left[k^2 - \frac{\sqrt{\lambda}''}{\sqrt{\lambda}} \right] f_{k,\alpha} = 0, \quad g_{k,\alpha}'' + \left[k^2 - \sqrt{\lambda} \left(\frac{1}{\sqrt{\lambda}} \right)'' \right] g_{k,\alpha} = 0, \quad (2.28)$$

which have the same content of Eq. (2.20) provided the initial conditions are correctly imposed by taking into account that $g_{k,\alpha}$ is ultimately determined from $f_{k,\alpha}$ and its derivative as $g_{k,\alpha} = f_{k,\alpha}' - \mathcal{F} f_{k,\alpha}$. Equations (2.20)–(2.28) are invariant under the following duality transformations⁵:

$$\sqrt{\lambda} \rightarrow 1/\sqrt{\lambda}, \quad f_{k,\alpha} \rightarrow g_{k,\alpha}/k, \quad g_{k,\alpha} \rightarrow -k f_{k,\alpha}. \quad (2.29)$$

³Equation (2.22) follows from Eqs. (2.18) and (2.19) by recalling that $\hat{B}_j(\vec{p}, \tau) = \int d^3x \hat{B}_j(\vec{x}, \tau) e^{i\vec{p}\cdot\vec{x}}/(2\pi)^{3/2}$ and that $\hat{E}_i(\vec{q}, \tau) = \int d^3x \hat{E}_i(\vec{x}, \tau) e^{i\vec{q}\cdot\vec{x}}/(2\pi)^{3/2}$.

⁴If the mode functions for the two polarizations coincide the sums appearing in Eqs. (2.25)–(2.26) can be performed trivially since $f_{k\oplus} = f_{k\otimes} = f_k$ and similarly for the hyperelectric mode function.

⁵In connection with Eqs. (2.20) and (2.29) we recall that $\mathcal{F} = \sqrt{\lambda}'/\sqrt{\lambda}$; this means that for $\sqrt{\lambda} \rightarrow 1/\sqrt{\lambda}$, $\mathcal{F} \rightarrow -\mathcal{F}$.

2.3 Spectral energy density and backreaction constraint

Since the amplification of the gauge fields takes place in a homogeneous and isotropic background geometry (see Eq. (2.8)) the corresponding energy density must not exceed the critical energy density $\rho_{crit} = 3 \bar{M}_P^2 H^2$ where H is the Hubble rate. The averaged energy density of the gauge fields follows from Eqs. (2.23) and (2.24) and from the definitions of ρ_B and ρ_E appearing in Eqs. (2.9), (2.10) and (2.11). Thanks to Eqs. (2.25)–(2.26) the final result is:

$$\langle \hat{\rho}_Y \rangle = \langle \hat{\rho}_B \rangle + \langle \hat{\rho}_E \rangle = \frac{1}{4\pi a^4(\tau)} \int \frac{dk}{k} \left[P_E(k, \tau) + P_B(k, \tau) \right]. \quad (2.30)$$

In terms of the physical power spectra of Eq. (2.27) the result (2.30) becomes:

$$\langle \hat{\rho}_Y \rangle = \frac{\lambda(\tau)}{4\pi} \int \frac{dk}{k} \left[P_E^{(phys)}(k, \tau) + P_B^{(phys)}(k, \tau) \right]. \quad (2.31)$$

To compare energy density of the parametrically amplified gauge fields with the energy density of the background geometry we introduce the spectral energy density in critical units:

$$\Omega_Y = \frac{1}{\rho_{crit}} \frac{d\langle \hat{\rho} \rangle}{d \ln k} = \frac{2}{3H^2 \bar{M}_P^2 a^4} \left[P_E(k, \tau) + P_B(k, \tau) \right]. \quad (2.32)$$

To guarantee the absence of dangerous backreaction effects $\Omega_Y(k, \tau)$ must always be much smaller 1 throughout all the stages of the evolution and for all relevant scales; this requirement must be separately verified both during and after inflation.

2.4 Gauge couplings and their continuity

2.4.1 Increasing gauge coupling

In Fig. 1 the profile describing the evolution of the gauge coupling is illustrated together with the main notations employed throughout the discussion. During the inflationary phase (i.e. for $\tau \leq -\tau_1$ in Fig. 1) γ

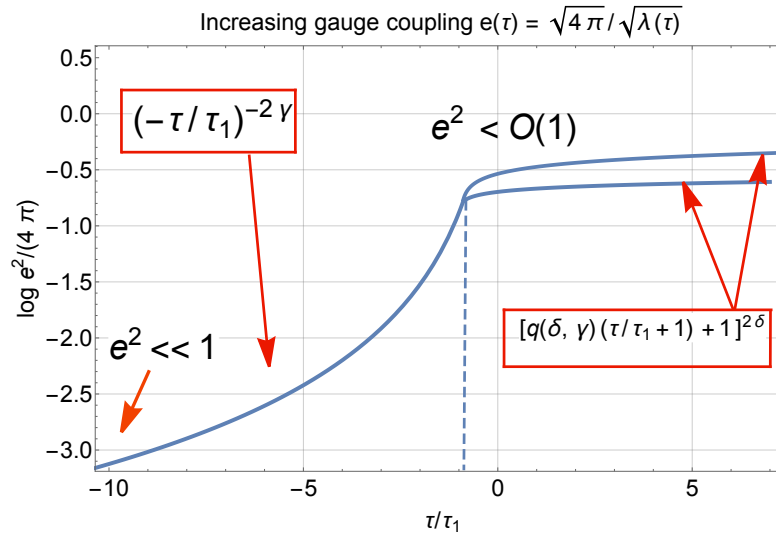


Figure 1: The logic and the main notations employed for the dynamical description of an increasing gauge coupling. The two different curves for $\tau \geq -\tau_1$ correspond to different values of $\delta \ll 1$. Note that $q(\delta, \gamma) = \delta/\gamma$ [see also Eq. (A.3)].

describes the rate of increase of the gauge coupling in the conformal time parametrization while δ controls the evolution during the post-inflationary stage of expansion when the gauge coupling flattens out:

$$\sqrt{\lambda} = \sqrt{\lambda_1} \left(-\frac{\tau}{\tau_1} \right)^\gamma, \quad \tau \leq -\tau_1, \quad (2.33)$$

$$\sqrt{\lambda} = \sqrt{\lambda_1} \left[\frac{\gamma}{\delta} \left(\frac{\tau}{\tau_1} + 1 \right) + 1 \right]^{-\delta}, \quad \tau \geq -\tau_1. \quad (2.34)$$

The explicit form of Eqs. (2.33) and (2.34) is dictated by the continuity of $\sqrt{\lambda}$ and of $\sqrt{\lambda}'$; furthermore the physical range of γ and δ is given by:

$$\gamma > 0, \quad \text{and} \quad 0 \leq \delta \ll \gamma. \quad (2.35)$$

For short the limit $\delta \rightarrow 0$ shall be referred to as the sudden approximation while the smooth approximation corresponds to the case of Eq. (2.35) where $0 \leq \delta \ll \gamma$. As we shall see it will always be possible to derive the results of the sudden approximation by taking the limit $\delta \rightarrow 0$ from the formulas valid in the case of the smooth approximation. The continuity of the magnetic and electric mode functions introduced in Eqs. (2.18)–(2.19) and obeying Eqs. (2.20)–(2.21) rely however on the continuity of $\sqrt{\lambda}$ and its derivative. If we would simply assume that $\sqrt{\lambda}$ is constant the conformal time derivative will have a jump discontinuity and Eq. (2.28) will develop a singularity either in $\sqrt{\lambda}''/\sqrt{\lambda}$ or in $(1/\sqrt{\lambda})''\sqrt{\lambda}$. Since the present approach guarantees the continuity of gauge mode functions the related power spectra will also be continuous. Note that the numerical value of λ_1 may well coincide with 1 but it could also be slightly larger than 1 since this range is compatible with a gauge coupling that is perturbative for $\tau = -\tau_1$, as illustrated in Fig. 1.

In the geometry of Eq. (2.8) the background equations derived from Eqs. (2.4)–(2.5) are:

$$3\bar{M}_P^2 \mathcal{H}^2 = \frac{1}{2}\varphi'^2 + a^2 W(\varphi), \quad 2\bar{M}_P^2 (\mathcal{H}^2 - \mathcal{H}') = \varphi'^2, \quad \varphi'' + 2\mathcal{H}\varphi' + \frac{\partial W}{\partial \varphi} a^2 = 0, \quad (2.36)$$

where, as already mentioned, the prime denotes a derivation with respect to the conformal time coordinate τ ; furthermore $\mathcal{H} = (\ln a)' = aH$ where $H = \dot{a}/a$ is the conventional Hubble rate and the overdot denotes a derivation with respect to the cosmic time coordinate t . The slow roll approximation specifies the evolution during the inflationary phase where the parameters ϵ , η and $\bar{\eta}$ are all much smaller than 1 and eventually get to 1 when inflation ends. The definitions of the slow roll parameters within the notations of this paper are as follows:

$$\epsilon = -\frac{\dot{H}}{H^2} = \frac{\bar{M}_P^2}{2} \left(\frac{W_{,\varphi}}{W} \right)^2, \quad \eta = \frac{\ddot{\varphi}}{H\dot{\varphi}}, \quad \bar{\eta} = \bar{M}_P^2 \left(\frac{W_{,\varphi\varphi}}{W} \right), \quad (2.37)$$

note that $W_{,\varphi}$ and $W_{,\varphi\varphi}$ are shorthand notations for the first and second derivatives of the potential $W(\varphi)$ with respect to φ . The slow roll parameters η , $\bar{\eta}$ and ϵ are not independent and their mutual relation, i.e. $\eta = \epsilon - \bar{\eta}$, follows from the slow roll version of Eqs. (2.36) written in the cosmic time coordinate t :

$$3H\dot{\varphi} + \frac{\partial W}{\partial \varphi} = 0, \quad 3\bar{M}_P^2 H^2 = W, \quad 2\bar{M}_P^2 \dot{H} = -\dot{\varphi}^2. \quad (2.38)$$

We shall be assuming that the inflationary stage of expansion takes place for $\tau \leq -\tau_1$:

$$\mathcal{H} = aH = -\frac{1}{(1-\epsilon)\tau}, \quad \epsilon = -\frac{\dot{H}}{H^2} \ll 1, \quad (2.39)$$

whereas after inflation (i.e. for $\tau \geq -\tau_1$) the background will be decelerated and dominated by radiation. The continuity of the scale factor demands:

$$\begin{aligned} a_{inf}(\tau) &= \left(-\frac{\tau}{\tau_1} \right)^{-\beta}, \quad \tau \leq -\tau_1, \\ a_{rad}(\tau) &= \frac{\tau + (\beta + 1)\tau_1}{\tau_1}, \quad \tau \geq -\tau_1. \end{aligned} \quad (2.40)$$

with $\beta \simeq 1/(1 - \epsilon)$. Both Eqs. (2.39) and (2.40) assume that ϵ changes very slowly during inflation. The continuity of the scale factor and of its conformal time derivative also imply the continuity of the extrinsic curvature whose background value is given by $\bar{K}_{ij} = -a \mathcal{H} \delta_{ij}$.

For a correct treatment of the problem the continuity of the extrinsic curvature is essential. However various other effects could be always added with the purpose of providing a more accurate description of the transition regime. For instance it could be observed that the slow-roll approximation breaks down at the end of inflation so that ϵ is not truly constant across the transition. Another possibility is represented by the dynamics of reheating. These situations will affect the maximal frequency of the spectrum which is therefore rather difficult to predict with great accuracy. This situation is actually analog to what happens in the case of the spectrum of relic gravitons [45]. In analogy with the graviton spectrum we shall therefore parametrize the maximal wavenumber as $k_{max} = \zeta a_1 H_1$ where ζ is a numerical factor which may even be, in some cases, dependent upon the wavenumber. The impact of the breakdown of the slow-roll approximation on the maximal frequency of the spectrum has been discussed in [46]. In the present case these considerations are anyway immaterial since the typical wavenumbers relevant for magnetogenesis are typically much smaller i.e. $\mathcal{O}(\text{Mpc}^{-1})$ as we shall see.

In a complementary perspective it should also be mentioned that the maximal frequency of the spectrum could be affected by the details of the reheating dynamics. As already suggested in the previous paragraph the continuity of the extrinsic curvature is an excellent starting point also in this case. More detailed models of reheating could be certainly useful and might affect the magnetogenesis scenarios (as suggested in [47]). In this paper we adopted the approximation of the sudden reheating which is also the one often employed in order to set limits on the tensor to scalar ratio and on the total number of inflationary e -folds. We shall however relax this approximation in phenomenological discussion of section 5.

2.4.2 Decreasing gauge coupling

For the purposes of the present analysis it is useful to complement the timeline of Fig. 1 with Fig. 2 describing the dual situation where the gauge coupling is initially much larger than 1. In the situation

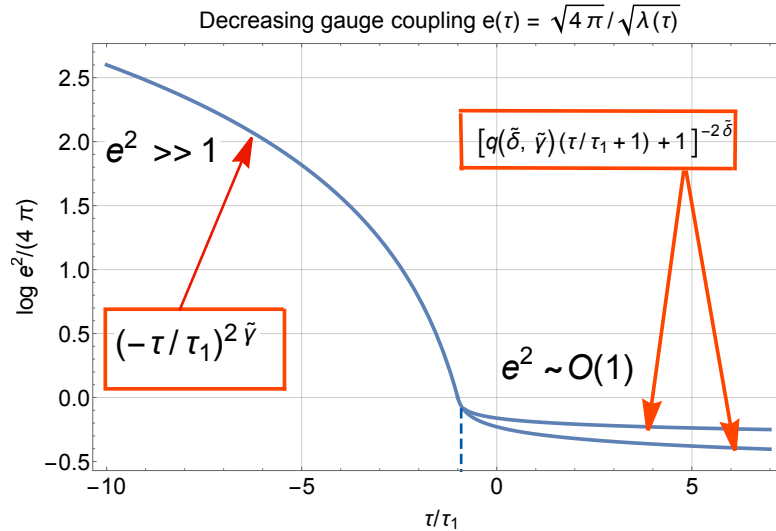


Figure 2: We illustrate the main notations employed when discussing the case of the decreasing gauge coupling. As in the case of Fig. 1 the two different curves for $\tau \geq -\tau_1$ correspond to different values of $\tilde{\delta} \ll 1$. Note that $q(\tilde{\delta}, \tilde{\gamma}) = \tilde{\delta} / \tilde{\gamma}$ [see also Eq. (B.4)].

illustrated by Fig. 2 the continuity of $\sqrt{\lambda}$ and $\sqrt{\lambda}'$ imply the following parametrization

$$\sqrt{\lambda} = \sqrt{\lambda_1} \left(-\frac{\tau}{\tau_1} \right)^{-\tilde{\gamma}}, \quad \tau < -\tau_1, \quad (2.41)$$

$$\sqrt{\lambda} = \sqrt{\lambda_1} \left[\frac{\tilde{\gamma}}{\tilde{\delta}} \left(\frac{\tau}{\tau_1} + 1 \right) + 1 \right]^{\tilde{\delta}}, \quad \tau \geq -\tau_1, \quad (2.42)$$

The physical region of the parameters is given by:

$$\tilde{\gamma} > 0, \quad \tilde{\delta} \geq 0, \quad \text{and} \quad 0 < \tilde{\delta} \ll \tilde{\gamma}. \quad (2.43)$$

The limit $\tilde{\delta} \rightarrow 0$ denotes again the sudden approximation while the smooth approximation holds for $\tilde{\delta} \ll 1$ or, which is the same, $\tilde{\delta} \ll \tilde{\gamma}$ since we shall assume throughout that $\tilde{\gamma}$ is of order 1. As in the case of increasing gauge coupling (see Eqs. (2.33)–(2.34)), Eqs. (2.41)–(2.42) will be complemented by the smooth evolution of the geometry illustrated in Eq. (2.40). The dual profiles of Figs. 1 and 2 are not physically equivalent. If we consider a certain reference time $\tau = -\tau_i$ close to the onset of the inflationary phase, we will have, according to Eq. (2.41) that

$$\sqrt{\lambda_i} = \sqrt{\lambda_1} \left(\frac{a_i}{a_f} \right)^{\tilde{\gamma}} \ll 1 \Rightarrow e(\tau_i) = \frac{\sqrt{4\pi}}{\sqrt{\lambda_i}} \gg 1, \quad (2.44)$$

where, by definition, $\lambda_i = \lambda(-\tau_i)$; in Eq. (2.44) we traded the conformal time for the scale factors by using Eq. (2.40) in the limit $\epsilon \ll 1$. Note in fact that $(a_i/a_f)^{\tilde{\gamma}} = e^{-N\tilde{\gamma}} \ll 1$ where N is the total number of inflationary e -folds. Since $N = \mathcal{O}(60)$ (or larger) we have that $\sqrt{\lambda_i}$ will be $\mathcal{O}(10^{-60})$ (or smaller). Equation (2.44) implies that the evolution of the gauge coupling starts from a non-perturbative regime unless $\sqrt{\lambda_1}$ is extremely large: only in this way we would have $\sqrt{\lambda_i} = \mathcal{O}(1)$. Whenever $\sqrt{\lambda_1} \gg 1$ the gauge coupling will be extremely minute at the end of inflation and this is at odds with the fact that during the decelerated stage of expansion we would like to have $e^2 = \mathcal{O}(10^{-2})$ but not much smaller. Furthermore, as we shall see in section 5, the physical power spectra are suppressed as λ_1^{-1} and this will make their contribution marginal for the phenomenological implications. A possibility suggested in Ref. [44] has been that the $\sqrt{\lambda}$ increases during inflation, decreases sharply during reheating, and then flattens out again. This suggestion is often assumed by various authors but rarely justified.

3 Inflationary gauge spectra and their constraints

The qualitative description of large-scale cosmological perturbations suggests that a given wavelength exits the Hubble radius at some typical conformal time during an inflationary stage of expansion and approximately reenters at $\tau_k \sim 1/k$, when the Universe still expands but in a decelerated manner. By a mode being beyond the horizon we only mean that the physical wavenumber is much less than the expansion rate: this does not necessarily have anything to do with causality [22, 41]. Similarly the physical wavenumbers of the hyperelectric and hypermagnetic fields can be much smaller than the rate of variation of the gauge coupling which now plays the role of the effective horizon. During inflation the relevant regime will be the one where the wavelengths of the gauge fluctuations are inside the effective horizon which means that $k/\mathcal{F} \simeq k\tau \ll 1$. As long as $k\tau < 1$ duality will be a valid symmetry but as soon as $k\tau_k \sim 1$ the electric spectra will be suppressed by conductivity and the gauge spectra will not be related by duality (see in this respect section 5). Not all the wavelengths that are larger than the effective horizon will reenter at the end of inflation (i.e. for $\tau = -\tau_1$) but throughout the whole radiation phase. Thus the gauge spectra for wavelengths larger than the effective horizon during inflation do not necessarily coincide with the gauge spectra when the given mode reenters (see, in this respect, section 4).

The logic of this section will be to compute the gauge spectra during inflation for the profiles schematically introduced in Figs. 1 and 2. We shall then demonstrate that the gauge power spectra in the two cases are explicitly related by duality. This will mean, for instance, that during inflation the generation of potentially scale-invariant hyperelectric spectrum is only compatible with a phase where the gauge coupling decreases while a flat hypermagnetic spectrum may only arise when the gauge coupling decreases.

3.1 Increasing gauge coupling

When $\sqrt{\lambda}$ is given by (2.33) the solution of Eq. (2.20) compatible with the Wronskian normalization dictated by Eq. (2.21) is given by⁶:

$$f_k(\tau) = \frac{N_\mu}{\sqrt{2k}} \sqrt{-k\tau} H_\mu^{(1)}(-k\tau), \quad \mu = \left| \gamma - \frac{1}{2} \right|, \quad (3.1)$$

$$g_k(\tau) = N_\mu \sqrt{\frac{k}{2}} \sqrt{-k\tau} H_{\mu+1}^{(1)}(-k\tau), \quad \gamma > \frac{1}{2}, \quad (3.2)$$

$$g_k(\tau) = -N_\mu \sqrt{\frac{k}{2}} \sqrt{-k\tau} H_{\mu-1}^{(1)}(-k\tau), \quad 0 < \gamma < \frac{1}{2}. \quad (3.3)$$

In general $H_\nu^{(1)}(z)$ will denote the Hankel functions first kind [42, 43] with argument z and index ν ; N_ν is a complex number whose phase is required for a correct asymptotic normalization of the mode functions:

$$H_\nu^{(1)}(z) = J_\nu(z) + iY_\nu(z), \quad N_\nu = \sqrt{\frac{\pi}{2}} e^{i\pi(2\nu+1)/4}. \quad (3.4)$$

Throughout the whole discussion we shall assume, as in the standard theory of Hankel functions [42, 43] that ν is real and positive semi-definite:

$$\text{Re } \nu \geq 0, \quad \text{Im } \nu = 0, \quad H_{-\nu}^{(1)}(z) = e^{i\pi\nu} H_\nu^{(1)}(z), \quad H_{-\nu}^{(2)}(z) = e^{-i\pi\nu} H_\nu^{(2)}(z). \quad (3.5)$$

Inserting the correctly normalized mode functions of Eqs. (3.1), (3.2) and (3.3) into Eqs. (2.25)–(2.26) the gauge spectra for $\tau \leq -\tau_1$ turn out to be⁷:

$$P_B(k, \tau) = \frac{a^4 H^4}{8\pi} (-k\tau)^5 |H_\mu^{(1)}(-k\tau)|^2 \rightarrow a^4 H^4 D(\mu) |k\tau|^{5-2\mu} \quad (3.6)$$

$$P_E(k, \tau) = \frac{a^4 H^4}{8\pi} (-k\tau)^5 |H_{\mu+1}^{(1)}(-k\tau)|^2 \rightarrow a^4 H^4 D(\mu+1) |k\tau|^{5-2(\mu+1)}, \quad \gamma > 1/2, \quad (3.7)$$

$$P_E(k, \tau) = \frac{a^4 H^4}{8\pi} (-k\tau)^5 |H_{\mu-1}^{(1)}(-k\tau)|^2 \rightarrow a^4 H^4 D(|\mu-1|) |k\tau|^{5-2|\mu-1|}, \quad 0 < \gamma < 1/2, \quad (3.8)$$

where we introduced the function:

$$D(x) = 2^{2x-3} \frac{\Gamma^2(x)}{\pi^3}, \quad (3.9)$$

that will be used throughout the whole paper exactly with the same meaning; the function $D(x)$ arises when the gauge spectra are evaluated outside the effective horizon (i.e. for $|k\tau| < 1$) and the corresponding Hankel functions are estimated using their limit for small arguments [42, 43]. Note, in this respect, that $(-k\tau)$ can also be expressed as⁸

$$(-k\tau) = \frac{k}{(1-\epsilon)aH} \simeq \frac{k}{aH} = \frac{k}{a_1 H} e^{-N}, \quad \epsilon \ll 1, \quad N = \ln \left(\frac{a}{a_1} \right). \quad (3.10)$$

⁶For $\gamma \rightarrow 1/2$, $\mu \rightarrow 0$ and, in this limit, Eqs. (3.2) and (3.3) coincide exactly since $H_{-1}^{(1)}(z) = e^{i\pi} H_1^{(1)}(z)$. See also Eq. (3.5).

⁷A term $|1-\epsilon|^4$ has been omitted in the prefactors since it coincides with 1 for $\epsilon \ll 1$.

⁸ N denotes the total number of inflationary e -folds and has nothing to do with the normalization N_μ of the mode functions.

Since, by definition, $\mu = |\gamma - 1/2|$ in terms of γ the comoving power spectra of Eqs. (3.6), (3.7) and (3.8) become:

$$P_B(k, \tau) = a^4 H^4 D(|\gamma - 1/2|) |k\tau|^{5-|2\gamma-1|}, \quad (3.11)$$

$$P_E(k, \tau) = a^4 H^4 D(\gamma + 1/2) |k\tau|^{4-2\gamma}. \quad (3.12)$$

The derivation of Eq. (3.11) from Eq. (3.6) is immediate from the definition of μ in terms of γ (i.e. $\mu = |\gamma - 1/2|$). On the contrary Eq. (3.12) is the common expression of Eqs. (3.7) and (3.8). In fact, in Eq. (3.7) $\mu = \gamma - 1/2$ (and therefore $\mu + 1 = \gamma + 1/2$), conversely in Eq. (3.8) $\mu = 1/2 - \gamma$ and $|\mu - 1|$ always equals $\gamma + 1/2$. After direct insertion of Eqs. (3.11)–(3.12) into Eq. (2.32) the spectral energy density for $\tau \leq -\tau_1$ is

$$\Omega_Y(k, \tau) = \frac{2}{3} \left(\frac{H}{M_P} \right)^2 \left[D_B(|\gamma - 1/2|) |k\tau|^{5-|2\gamma-1|} + D_E(\gamma + 1/2) |k\tau|^{4-2\gamma} \right]. \quad (3.13)$$

The spectral energy density of Eq. (3.13) must be always subcritical (i.e. $\Omega_Y(k, \tau) \ll 1$) for $\tau \leq -\tau_1$ and $|k\tau| \leq 1$; this requirement is not always satisfied even if, during the inflationary phase, $H \ll M_P$. The first term inside the square bracket at the right hand side of Eq. (3.13) denotes the magnetic contribution while the second term is the electric result⁹. By looking together at Eqs. (3.11), (3.12) and (3.13) the following conclusions naturally emerge:

- if $\gamma = 2$ the hyperelectric spectrum is exactly scale-invariant while the magnetic spectrum is steeply increasing [i.e. $P_B(k, \tau) \propto |k\tau|^2$ for $k\tau \ll 1$] so that the condition $\Omega_Y(k, \tau) \ll 1$ is safely satisfied;
- if $1/2 < \gamma \leq 2$ the requirement $\Omega_Y(k, \tau) \ll 1$ always holds for $|k\tau| \ll 1$ but, according to the general wisdom, the magnetogenesis constraints cannot be satisfied since the hypermagnetic power spectrum is still too violet;
- if $\gamma > 2$ the hypermagnetic spectrum becomes even steeper while the hyperelectric spectrum diverges in the limit $k\tau \ll 1$: in this case the bound $\Omega_Y \ll 1$ is not satisfied so that the whole class of models $\gamma > 2$ must be excluded.

The only case not explicitly covered is $\gamma \rightarrow 1/2$ but in this case both the electric and the magnetic spectra are steeply increasing while the magnetic spectrum inherits a logarithmic correction¹⁰:

$$P_B(k, \tau) = \frac{a^4 H^4}{8\pi} (-k\tau)^5 |H_0^{(1)}(-k\tau)|^2 \rightarrow \frac{a^4 H^4}{2\pi^3} |k\tau|^5 \ln^2 |k\tau|, \quad (3.14)$$

$$P_E(k, \tau) = \frac{a^4 H^4}{8\pi} (-k\tau)^5 |H_1^{(1)}(-k\tau)|^2 \rightarrow \frac{a^4 H^4}{2\pi^3} |k\tau|^3, \quad (3.15)$$

$$\Omega_Y(k, \tau) = \frac{1}{3\pi^3} \left(\frac{H}{M_P} \right)^2 |k\tau|^3 \left[1 + |k\tau|^2 \ln^2 |k\tau| \right]. \quad (3.16)$$

Therefore, also in the case $\gamma \rightarrow 1/2$ the spectral energy density is subcritical when the typical wavelengths are larger than the effective horizon.

If we consider Eq. (3.13) at face value we must admit that for $\gamma \leq 2$ the critical density constraint is always satisfied since both the hyperelectric and the hypermagnetic power spectra are extremely minute; the relation among them can be easily deduced from Eqs. (3.11)–(3.12) and it is given by:

$$P_B(k, \tau) = (-k\tau)^2 P_E(k, \tau), \quad \text{for } \gamma > 1/2, \quad (3.17)$$

$$P_B(k, \tau) = (-k\tau)^{4\gamma} P_E(k, \tau), \quad \text{for } 0 < \gamma < 1/2. \quad (3.18)$$

⁹To stress this we just added a subscript to the function $D(x)$ (by writing $D_B(x)$ and $D_E(x)$) even if the definition of $D(x)$ (see after Eq. (3.8)) is the same in both cases.

¹⁰When $\gamma \rightarrow 1/2$ the mode functions become $f_k(\tau) = N_0 \sqrt{-k\tau} H_0^{(1)}(-k\tau)/\sqrt{2k}$ and $g_k(\tau) = N_0 \sqrt{k/2} \sqrt{-k\tau} H_1^{(1)}(-k\tau)$, where $N_0 = \sqrt{\pi/2} e^{i\pi/4}$.

In both cases the hypermagnetic field spectrum is smaller than its hyperelectric counterpart. This feature may also arise in other models but it is not problematic as long as the power spectra are both very small. There have been recently various suggestions attempting to include spectator (electric) fields in curved backgrounds [48, 49] with the purpose of estimating the Schwinger effect in de Sitter space-time. These estimates are typically done by assuming a constant and uniform electric field in de Sitter space and by also postulating a vector-like coupling to fermions. These three assumptions do not specifically hold in the present case since the fields obtained here are non-uniform and non-homogeneous, they are not constant in time and they have, in general, a chiral coupling to fermions.

It is interesting to note that the estimates of the Schwinger-like effects are highly non-generic in the sense that to have a sizeable effect we need to concoct specific currents forbidding the dilution of the electric energy density by the expansion of the universe. Indeed, the constancy and uniformity of the field configurations entering the estimate of the above effect is achieved by considering a class of appropriate currents and this physical situation is markedly different from the flat space-time case where the constancy and uniformity of the field imposes the absence of time-dependent currents. The idea of Refs. [48] (somehow questioned in Ref. [49]) is that to achieve a physical electric field that is constant¹¹ one must actually require the presence of a comoving current so that the explicit form of the corresponding evolution equations will be:

$$\nabla \times \vec{E} = 0, \quad \nabla \times \vec{B} = 0, \quad \vec{J} + \vec{E}' = 0, \quad \vec{B}' = 0. \quad (3.19)$$

If one would simply choose $\vec{E} = E_0 \hat{n}$ (where \hat{n} is a certain unit vector), $\vec{B} = 0$ and $\vec{J} = 0$ this would be the standard Schwinger ansatz but the rate of pair production in de Sitter space would be negligible since the physical fields will be suppressed as $\vec{E}^{(phys)} = E_0 \hat{n}/a^2$. To have a non-negligible effect the common wisdom is therefore to postulate an *ad hoc* current constructed in such a way that the resulting *physical field* is a space-time constant. This can be achieved by postulating a comoving field in the form $\vec{E} = a^\lambda E_0 \hat{n}$ [49] implying that the corresponding current becomes, from Eq. (3.19), $\vec{J} = -\lambda a H \vec{E}$. If $\lambda \leq 2$ the corresponding physical field is less suppressed and it becomes constant in the limit $\lambda \rightarrow 2$. These spectator electric fields can be understood as the result of an effective conductivity $\sigma = -\lambda H a$ which is negative if the universe expands (as we are discussing here). It has been argued that this approach may cause a violation of the second law of thermodynamics [49]. It is debatable if this kind of estimates are at all relevant for the situation described in this paper. Even assuming that the coupling of hypercharge fields is vector-like (which is not the case as discussed above), the effects of the current $\vec{J} = -\lambda a H \vec{E}$ are physically quite different from the ones associated with the spectra (3.17)–(3.18) which are fully inhomogeneous, time-dependent and obtained in the absence of *any* supporting current.

Having specified what is the real physical situation we can always try to see under which conditions the probability of pair creation per unit volume per unit time is under control in some averaged sense. Taking into account all the preceding caveats, and denoting with Γ the rate of pair production per unit volume and per unit time a reasonable condition to consider seems to be:

$$\frac{\Gamma}{H^4} = \frac{\alpha}{\pi^2} \langle E^2(\tau, \vec{x}) \rangle < 1, \quad \Rightarrow \frac{2}{\pi^2 \lambda} \int_0^{k_{max}} \frac{dk}{k} P_E(k, \tau) < H^4, \quad (3.20)$$

where we recalled that, within the conventions spelled out in Eq. (2.17), $\alpha = e^2/(4\pi) = 1/\lambda$; we also assumed that the flat-space result holds (locally) over typical scales $\mathcal{O}(H^{-1})$ during the quasi-de Sitter stage. Let us now consider, for simplicity, the case of Eq. (3.17) and see if and how the condition (3.20) is satisfied. In Eq. (3.20) k_{max} denotes the maximally amplified wavenumber which is given, in the present context $k_{max} = \mathcal{O}(1/\tau_1)$. By using the explicit form of the power spectrum given in Eq. (3.12) the condition (3.20) implies

$$\frac{e_1^2 2^{2\gamma-3} \Gamma^2(\gamma + 1/2) \zeta^{4-2\gamma} \left(\frac{a_1}{a}\right)^{-4\gamma}}{(4-2\gamma)\pi^5} \ll 1, \quad 0 < \gamma < 2, \quad (3.21)$$

¹¹It turns out to be useful, in this respect, the distinction between physical and comoving fields given in Eqs. (2.12). The only caveat is that, in standard estimates of the Schwinger effect, the gauge coupling does not evolve.

where ζ is a numerical factor $\mathcal{O}(1)$ [we parametrized $k_{max} = \zeta/\tau_1$ by following the observations discussed after Eq. (2.40)]. The condition Eq. (3.21) is always verified for $\tau < -\tau_1$ since in the wanted range of γ we have that $(a_1/a)^{-4\gamma} = (-\tau/\tau_1)^{-4\gamma} \ll 1$. This suggests that the condition (3.21) is always satisfied except, probably, at the very end of inflation. This is, however, not a problem of the physics but just a problem of the accuracy in the estimate of the inflationary spectrum around k_{max} . Even in the worse situation the ideas conveyed in this paper come do not contradict the spirit of the bound (3.21): since the gauge coupling at the end of inflation is effectively a tuneable parameter, it is sufficient to reduce e_1^2 by one order of magnitude to safely satisfy the conditions (3.20) and (3.21) also at the end of inflation. All in all Eqs. (3.19)–(3.20) and (3.21) suggest that the constraints coming from pair production are therefore not essential in the present context even if an improved understanding of the whole problem would be desirable (see e.g. [49]) and discussions therein).

In summary when the gauge coupling increases during a quasi-de Sitter stage of expansion the spectral energy density is subcritical for $0 < \gamma \leq 2$ and overcritical for $\gamma > 2$ so that the latter range is excluded while the former is still viable. Since the hypermagnetic spectrum is rather steep (i.e. violet) when $\gamma = 2$ the conventional wisdom is that it will also be minute at the galactic scale after the gauge coupling flattens out. This swift conclusion is only true provided the hypermagnetic magnetic power spectrum at the end of inflation is not modified for $\tau \geq -\tau_1$. In section 4 the gauge power spectra will be explicitly computed in the regime where the gauge coupling flattens out (i.e. for $\tau \geq -\tau_1$) and it will be shown that the late-time hypermagnetic spectrum does not coincide with the hypermagnetic spectrum at the end of inflation when the gauge coupling increases.

3.2 Decreasing gauge coupling

When $\sqrt{\lambda}$ evolves as in Eq. (2.41) (see also Fig. 2) the correctly normalized solution of Eqs. (2.20) and (2.21) are now given by

$$f_k(\tau) = \frac{N_{\tilde{\mu}}}{\sqrt{2k}} \sqrt{-k\tau} H_{\tilde{\mu}}^{(1)}(-k\tau), \quad g_k(\tau) = N_{\tilde{\mu}} \sqrt{\frac{k}{2}} \sqrt{-k\tau} H_{\tilde{\mu}-1}^{(1)}(-k\tau), \quad (3.22)$$

where

$$\tilde{\mu} = \tilde{\gamma} + \frac{1}{2}, \quad N_{\tilde{\mu}} = \sqrt{\frac{\pi}{2}} e^{i\pi(2\tilde{\mu}+1)/4}. \quad (3.23)$$

Inserting Eqs. (3.22) and (3.23) into Eqs. (2.25) and (2.26) the comoving power spectra are:

$$\widetilde{P}_B(k, \tau) = \frac{a^4 H^4}{8\pi} (-k\tau)^5 |H_{\tilde{\mu}}^{(1)}(-k\tau)|^2 \rightarrow a^4 H^4 D(\tilde{\mu}) |k\tau|^{5-2\tilde{\mu}}, \quad (3.24)$$

$$\widetilde{P}_E(k, \tau) = \frac{a^4 H^4}{8\pi} (-k\tau)^5 |H_{\tilde{\mu}-1}^{(1)}(-k\tau)|^2 \rightarrow a^4 H^4 D(|\tilde{\mu}-1|) |k\tau|^{5-2|\tilde{\mu}-1|}, \quad (3.25)$$

where the function $D(x)$ has been already defined in Eq. (3.9) for a generic argument x . To stress that the power spectra (3.24)–(3.25) correspond to the case of decreasing gauge coupling a tilde has been added on top of each expression. Since, according to Eq. (3.23), $\tilde{\mu} = \tilde{\gamma} + 1/2$, Eqs. (3.24) and (3.25) are directly expressible in terms of $\tilde{\gamma}$ and the result is:

$$\widetilde{P}_B(k, \tau) = a^4 H^4 D(\tilde{\gamma} + 1/2) |k\tau|^{4-2\tilde{\gamma}}, \quad (3.26)$$

$$\widetilde{P}_E(k, \tau) = a^4 H^4 D(|\tilde{\gamma} - 1/2|) |k\tau|^{5-|2\tilde{\gamma}-1|}. \quad (3.27)$$

Equations (3.26)–(3.27) will now be inserted into Eq. (2.32); the explicit expression of the spectral energy density is:

$$\widetilde{\Omega}_Y(k, \tau) = \frac{2}{3} \left(\frac{H}{M_P} \right)^2 \left[D_B(\tilde{\gamma} + 1/2) |k\tau|^{4-2\tilde{\gamma}} + D_E(|\tilde{\gamma} - 1/2|) |k\tau|^{5-|2\tilde{\gamma}-1|} \right], \quad (3.28)$$

where in analogy with Eq. (3.13) the subscripts E and B have been added to the function $D(x)$ with the purpose of reminding that the origin of the corresponding terms. As in the case of Eq. (3.13) the spectral energy density of Eq. (3.28) should always be subcritical (i.e. $\tilde{\Omega}_Y(k, \tau) \ll 1$ for $\tau \leq -\tau_1$ and $|k\tau| \ll 1$). In this respect the following three observations are in order:

- when $\tilde{\gamma} = 2$ the hypermagnetic spectrum is flat while the hyperelectric spectrum is violet and it goes as $\tilde{P}_E(k, \tau) \propto |k\tau|^2$; the spectral energy density is always subcritical for $|k\tau| \ll 1$;
- if $\tilde{\gamma} = 3$ the hyperelectric spectrum is flat however the hypermagnetic power spectrum diverges as $|k\tau|^{-2}$ in the limit $|k\tau| \ll 1$ but, in this case, the spectral energy density constraint is not satisfied;
- in the $0 < \tilde{\gamma} < 1/2$ the power spectra are both violet; all in all we conclude that the bound (3.28) is satisfied for $0 < \tilde{\gamma} \leq 2$.

The case $\tilde{\gamma} \rightarrow 1/2$ is not explicitly covered by Eq. (3.28) so that, in this limit, we have¹²

$$\tilde{P}_B(k, \tau) = \frac{a^4 H^4}{8\pi} (-k\tau)^5 |H_1^{(1)}(-k\tau)|^2 \rightarrow \frac{a^4 H^4}{2\pi^3} |k\tau|^3, \quad (3.29)$$

$$\tilde{P}_E(k, \tau) = \frac{a^4 H^4}{8\pi} (-k\tau)^5 |H_0^{(1)}(-k\tau)|^2 \rightarrow \frac{a^4 H^4}{2\pi^3} |k\tau|^5 \ln^2 |k\tau|, \quad (3.30)$$

$$\tilde{\Omega}_Y(k, \tau) = \frac{1}{3\pi^3} \left(\frac{H}{M_P} \right)^2 |k\tau|^3 \left[1 + |k\tau|^2 \ln^2 |k\tau| \right]. \quad (3.31)$$

3.3 Duality and gauge power spectra during inflation

A flat hypermagnetic spectrum is only consistent with the critical density bound provided $\tilde{\gamma} = 2$ (i.e. only when the gauge coupling is decreasing). Conversely a flat hyperelectric spectrum is only viable when the gauge coupling increases and $\gamma = 2$. Overall the only intervals where the critical density constraint is satisfied are given by $0 \leq \gamma \leq 2$ and $0 \leq \tilde{\gamma} \leq 2$. These results follow in fact from the duality symmetry of Eqs. (2.16) and (2.29). For the gauge spectra during inflation the duality symmetry implies, in general:

$$\sqrt{\lambda} \rightarrow \frac{1}{\sqrt{\lambda}}, \quad P_B(k, \tau) \rightarrow \tilde{P}_E(k, \tau), \quad P_E(k, \tau) \rightarrow \tilde{P}_B(k, \tau) \quad (3.32)$$

If now Eqs. (3.11)–(3.12) are compared with Eqs. (3.26)–(3.27) the spectra with increasing and decreasing gauge coupling during inflation are explicitly related by the following transformation:

$$\gamma \rightarrow \tilde{\gamma}, \quad P_B(k, \tau) \rightarrow \tilde{P}_E(k, \tau), \quad P_E(k, \tau) \rightarrow \tilde{P}_B(k, \tau). \quad (3.33)$$

Equation (3.33) has actually the same content of Eq. (3.32) since, according to the explicit parametrizations of Eqs. (2.33) and (2.41), the expression of $\sqrt{\lambda}$ is actually inverted when $\gamma \rightarrow \tilde{\gamma}$. Thanks Eq. (3.33) the spectral energy density is left invariant [i.e. $\Omega_Y(k, \tau) \rightarrow \tilde{\Omega}_Y(k, \tau)$] since the hyperelectric and the hypermagnetic power spectra are interchanged. All in all the standard lore stipulates that the only phenomenologically relevant case is the one $\tilde{\gamma} = 2$ since the other cases lead to an hypermagnetic spectrum that is either too steep or anyway inconsistent with the critical density bound. As already mentioned, this statement assumes that the gauge spectra are unmodified when coupling flattens out and the relevant wavelengths are still larger than the effective horizon.

¹²When $\tilde{\gamma} = 1/2$ the solution of Eqs. (2.20)–(2.21) is given by $f_k(\tau) = N_1 \sqrt{-k\tau} H_1^{(1)}(-k\tau)/\sqrt{2k}$ and by $g_k(\tau) = -N_1 \sqrt{\frac{k}{2}} \sqrt{-k\tau} H_0^{(1)}(-k\tau)$.

4 Post-inflationary gauge spectra and continuity

When the gauge coupling flattens out as illustrated in Figs. 1 and 2 the background geometry enters a stage of decelerated expansion after the end of the inflationary phase. The post-inflationary gauge fields are determined by the continuous evolution of the corresponding mode functions whose late-time behaviour follows from the elements of an appropriate transition matrix mixing together the hyperelectric and the hypermagnetic mode functions at the end of inflation and leading to specific standing oscillations. These Sakharov phases are different for the (γ, δ) transition illustrated in Fig. 1 and in the case of the $(\tilde{\gamma}, \tilde{\delta})$ profile of Fig. 2.

4.1 Increasing gauge coupling

4.1.1 Mixing matrix for the (γ, δ) transition

The continuous parametrization of $\sqrt{\lambda}$ given in Eqs. (2.33) and (2.34) implies that the late-time values of $f_k(\tau)$ and $g_k(\tau)$ for $\tau \geq -\tau_1$ are given by:

$$\begin{pmatrix} f_k(\tau) \\ g_k(\tau)/k \end{pmatrix} = \begin{pmatrix} A_{ff}(k, \tau, \tau_1) & A_{fg}(k, \tau, \tau_1) \\ A_{gf}(k, \tau, \tau_1) & A_{gg}(k, \tau, \tau_1) \end{pmatrix} \begin{pmatrix} \bar{f}_k \\ \bar{g}_k/k \end{pmatrix}, \quad (4.1)$$

where $\bar{f}_k = f_k(-\tau_1)$ and $\bar{g}_k = g_k(-\tau_1)$ denote the values of the mode functions at end of the inflationary phase and the matrix elements at the right hand side of Eq. (4.1) are determined from the continuity of the mode functions as described in appendix A:

$$\begin{aligned} A_{ff}(k, \tau, \tau_1) &= \frac{\pi}{2} \sqrt{qx_1} \sqrt{ky} \left[Y_{\nu-1}(qx_1) J_{\nu}(ky) - J_{\nu-1}(qx_1) Y_{\nu}(ky) \right], \\ A_{fg}(k, \tau, \tau_1) &= \frac{\pi}{2} \sqrt{qx_1} \sqrt{ky} \left[J_{\nu}(qx_1) Y_{\nu}(ky) - Y_{\nu}(qx_1) J_{\nu}(ky) \right], \\ A_{gf}(k, \tau, \tau_1) &= \frac{\pi}{2} \sqrt{qx_1} \sqrt{ky} \left[Y_{\nu-1}(qx_1) J_{\nu-1}(ky) - J_{\nu-1}(qx_1) Y_{\nu-1}(ky) \right], \\ A_{gg}(k, \tau, \tau_1) &= \frac{\pi}{2} \sqrt{qx_1} \sqrt{ky} \left[J_{\nu}(qx_1) Y_{\nu-1}(ky) - Y_{\nu}(qx_1) J_{\nu-1}(ky) \right]. \end{aligned} \quad (4.2)$$

Since the inflationary mode functions \bar{f}_k and \bar{g}_k obey the Wronskian normalization of Eq. (2.21), also $f_k(\tau)$ and $g_k(\tau)$ must obey the same condition for $\tau \geq \tau_1$ and this happens provided¹³:

$$A_{ff}(k, \tau, \tau_1) A_{gg}(k, \tau, \tau_1) - A_{fg}(k, \tau, \tau_1) A_{gf}(k, \tau, \tau_1) = 1. \quad (4.3)$$

The arguments of the Bessel functions appearing in (4.2) depend on qx_1 and ky while the corresponding indices depend on δ ; the explicit expressions of q , y and ν are:

$$q(\delta, \gamma) = \frac{\delta}{\gamma}, \quad y(\tau, \delta, \gamma) = \tau + \tau_1 [1 + q(\delta, \gamma)], \quad \nu(\delta) = \delta + 1/2. \quad (4.4)$$

Equation (4.4) shows that, within the present notations, $y(-\tau_1) = q\tau_1$ which also implies (by definition of x_1) that $ky(-\tau_1) = qk\tau_1 = qx_1$. Consequently, as expected from the continuity of the mode functions,

$$A_{fg}(k, -\tau_1, \tau_1) = A_{gf}(k, -\tau_1, \tau_1) = 0, \quad A_{ff}(k, -\tau_1, \tau_1) = A_{gg}(k, -\tau_1, \tau_1) = 1. \quad (4.5)$$

Since all the expression entering Eq. (4.2) ultimately depend on the dimensionless variables $x = k\tau$, $x_1 = k\tau_1$ and ν , the matrix appearing in Eq. (4.1) is in fact a function of δ , x and x_1 for any fixed value of γ :

$$\mathcal{M}(\delta, x, x_1) = \begin{pmatrix} A_{ff}(\delta, x, x_1) & A_{fg}(\delta, x, x_1) \\ A_{gf}(\delta, x, x_1) & A_{gg}(\delta, x, x_1) \end{pmatrix}. \quad (4.6)$$

¹³The validity of this condition can also be verified by plugging the explicit matrix elements of Eq. (4.2) into Eq. (4.3) and by using the standard recurrence relations involving the Bessel functions and their Wronskians [42, 43].

We stress that the variable $x_1 = k\tau_1 \leq 1$ measures k in units of the maximal wavenumber of the spectrum (i.e. $1/\tau_1 = a_1 H_1$) and this is why it cannot be larger than $\mathcal{O}(1)$.

4.1.2 General form of the power spectra

When the mode functions $f_k(\tau)$ and $g_k(\tau)$ are deduced from Eq. (4.1) the gauge power spectra of Eqs. (2.25)–(2.26) become:

$$P_B(k, \tau) = \frac{k^5}{2\pi^2} \left| A_{ff} \bar{f}_k + A_{fg} \frac{\bar{g}_k}{k} \right|^2, \quad (4.7)$$

$$P_E(k, \tau) = \frac{k^3}{2\pi^2} \left| k A_{gf} \bar{f}_k + A_{gg} \bar{g}_k \right|^2. \quad (4.8)$$

One of the two terms inside each of the squared moduli appearing in Eqs. (4.7) and (4.8) will be alternatively dominant. For the sake of concreteness we shall now verify that the first term inside the squared modulus of Eq. (4.7) dominates against the second:

$$\left| A_{fg}(\delta, x, x_1) \frac{\bar{g}_k}{k} \right| \gg \left| A_{ff}(\delta, x, x_1) \bar{f}_k \right|. \quad (4.9)$$

Since all the variables have been explicitly defined, the validity of the condition (4.9) could be investigated numerically¹⁴. For a more general proof of Eq. (4.9) it is sufficient to consider Eq. (4.9) in the limit $x_1 < 1$ (which is always verified for all the amplified modes of the spectrum) together with the subsidiary condition that $0 \leq \delta \ll \gamma$. An equivalent form of Eq. (4.9) and the result is:

$$\left| J_\nu(qx_1)Y_\nu(ky) - Y_\nu(qx_1)J_\nu(ky) \right| \gg \left| \frac{H_{|\gamma-1/2|}^{(1)}(x_1)}{H_{\gamma+1/2}^{(1)}(x_1)} \right| \left| Y_{\nu-1}(qx_1)J_\nu(ky) - J_{\nu-1}(qx_1)Y_\nu(ky) \right|. \quad (4.10)$$

If $x_1 \ll x \ll 1$ the arguments of the Bessel and Hankel functions appearing in Eq. (4.10) are all smaller than 1. It then follows that, in this limit (i.e. $x_1/x = \tau_1/\tau \ll 1$), the inequalities (4.9)–(4.10) are verified provided:

$$\left(\frac{qx_1}{2} \right)^{-2\delta} \gg \frac{\Gamma(1/2 - \delta)\Gamma(|\gamma - 1/2|)}{\Gamma(1/2 + \delta)\Gamma(\gamma + 1/2)} \left(\frac{x_1}{2} \right)^{\gamma+1/2-|\gamma-1/2|}, \quad (4.11)$$

where we used the explicit result of Eq. (A.9). When $\gamma > 1/2$ the condition (4.11) implies, up to irrelevant numerical factors, that $(qx_1/2)^{-2\delta} > (x_1/2)$ which is always verified¹⁵ as long as $x_1 < 1$ and $\delta \geq 0$. Similarly, if $0 < \gamma < 1/2$, Eq. (4.11) implies $(qx_1/2)^{-2\delta} > (x_1/2)^\gamma$ which is also verified in the physical range of the parameters.

So far we demonstrated that Eq. (4.9) holds in the range $x_1 \ll x \ll 1$. When $x_1 \ll 1$ and $x \gg 1$ the functions whose argument coincides with $ky \simeq x \gg 1$ can be always represented as¹⁶:

$$J_\nu(ky) = M_\nu \cos \theta_\nu, \quad Y_\nu(ky) = M_\nu \sin \theta_\nu, \quad (4.12)$$

where, for $x \gg 1$, $\theta_\nu(x) \rightarrow x$ while $M_\nu(x) \rightarrow \sqrt{2/\pi} x^{-1/2} [1 + \mathcal{O}(x^{-2})]$; this is the so-called modulus-phase approximation for the Bessel functions [42, 43]. Inserting Eq. (4.12) into Eq. (4.10) and expanding the

¹⁴This analysis has been performed by fixing γ to a reference value and by scanning the relative weight of the two terms of Eq. (4.9) for different values of $\delta \ll \gamma$. For the sake of conciseness this numerical analysis will not be explicitly discussed.

¹⁵In the limit $\delta \rightarrow 0$, since $q = \delta/\gamma$, the condition $(qx_1/2)^{-2\delta} \gg (x_1/2)$ is also verified as long as $x_1 < 1$. Since the gauge coupling freezes (either partially or totally) for $\tau > -\tau_1$ the physical situation discussed here corresponds to a range of parameters where $0 \leq \delta \ll 1/2$ which also implies $0 \leq \delta \ll \gamma$; these two conditions will be used interchangeably.

¹⁶Recall, in this respect, Eq. (4.4). Even if the value of x can be either smaller or larger than 1, as soon as $x = k\tau = \mathcal{O}(1)$ the conductivity cannot be neglected and this situation will be more specifically discussed in section 5. For the moment we shall just consider the case $x \gg 1$ as a mere mathematical limit.

remaining functions for $x_1 \ll 1$ it then follows that the inequality (4.9) is satisfied. Consequently, thanks to Eq. (4.9) the comoving spectrum of Eq. (4.7) is:

$$P_B(k, \tau) = \frac{k^5}{2\pi^2} \left| A_{fg}(\delta, x_1, x) \frac{\bar{g}_k}{k} \right|^2. \quad (4.13)$$

The results of Eqs. (4.9)–(4.13) show that the hyperelectric field at the end of inflation determines the late-time hypermagnetic field for $\tau \gg -\tau_1$. This is of course not a general truism but it happens provided the gauge coupling first increases during inflation and then flattens out in the radiation-dominated epoch. For the hyperelectric spectrum of Eq. (4.8) the inequality of Eq. (4.9) is in fact replaced by the following condition

$$\left| A_{gg}(\delta, x, x_1) \bar{g}_k \right| \gg \left| A_{gf}(\delta, x, x_1) k \bar{f}_k \right|, \quad (4.14)$$

which can be verified explicitly by using the same strategy illustrated in the case of Eq. (4.9); for the sake of conciseness these details will not be explicitly discussed. Therefore, thanks to Eq. (4.14), the late-time expression of the comoving hyperelectric spectrum is:

$$P_E(k, \tau) = \frac{k^3}{2\pi^2} \left| A_{gf}(\delta, x_1, x) \bar{g}_k \right|^2. \quad (4.15)$$

Equation (4.15) mirrors the result of Eq. (4.13) and it shows that the the hyperelectric power spectrum for $\tau \gg -\tau_1$ is determined by the hyperelectric power spectrum at $\tau = -\tau_1$. As we shall see in a moment when the gauge coupling decreases the dual result will hold.

4.1.3 Explicit expressions of the power spectra in various regimes

To obtain a more explicit form of the gauge power spectra in the decelerated stage of expansion the matrix elements of Eq. (4.2) can be expanded in powers of $x_1 \ll 1$. The strategy will be to fix ky and expand the various terms in powers of x_1 with the subsidiary conditions $0 \leq \delta \ll 1/2$. With these specifications Eq. (4.2) implies¹⁷:

$$A_{ff}(\delta, x_1, x) = \left(\frac{qx_1}{2} \right)^\delta \left[\sqrt{\frac{x}{2}} \Gamma(1/2 - \delta) J_{-\delta-1/2}(x) + \mathcal{O}(x_1) \right] + \mathcal{O}\left[(qx_1)^{1-\delta}\right], \quad (4.16)$$

$$A_{fg}(\delta, x_1, x) = \left(\frac{qx_1}{2} \right)^{-\delta} \left[\sqrt{\frac{x}{2}} \Gamma(1/2 + \delta) J_{\delta+1/2}(x) + \mathcal{O}(x_1) \right] + \mathcal{O}\left[(qx_1)^{1+\delta}\right], \quad (4.17)$$

$$A_{gf}(\delta, x_1, x) = \left(\frac{qx_1}{2} \right)^\delta \left[-\sqrt{\frac{x}{2}} \Gamma(1/2 - \delta) J_{1/2-\delta}(x) + \mathcal{O}(x_1) \right] + \mathcal{O}\left[(qx_1)^{1-\delta}\right], \quad (4.18)$$

$$A_{gg}(\delta, x_1, x) = \left(\frac{qx_1}{2} \right)^{-\delta} \left[\sqrt{\frac{x}{2}} \Gamma(1/2 + \delta) J_{\delta-1/2}(x) + \mathcal{O}(x_1) \right] + \mathcal{O}\left[(qx_1)^{1+\delta}\right]. \quad (4.19)$$

Thanks to the results of Eqs. (4.16)–(4.17) the inequality Eq. (4.9) can be again verified in a different manner. Furthermore, inserting Eq. (4.17) into Eq. (4.13) and recalling the expressions for \bar{f}_k and \bar{g}_k in the case of increasing coupling (see e.g. Eq. (A.8)) the hypermagnetic power spectrum becomes:

$$\begin{aligned} P_B(k, \tau) &= a_1^4 H_1^4 D(\gamma + 1/2) \left(\frac{k}{a_1 H_1} \right)^{4-2\gamma-2\delta} F_B(k\tau, \delta), \\ F_B(x, \delta) &= \left(\frac{q}{2} \right)^{-2\delta} \left(\frac{x}{2} \right) \Gamma^2(\delta + 1/2) J_{\delta+1/2}^2(x). \end{aligned} \quad (4.20)$$

¹⁷According to Eq. (4.4), $ky = x + x_1(q+1)$ and, to lowest order in x_1 , we have that $ky = x + \mathcal{O}(x_1)$.

Similarly, from Eq. (4.15) and (4.19) the hyperelectric spectrum turns out to be

$$\begin{aligned} P_E(k, \tau) &= a_1^4 H_1^4 D(\gamma + 1/2) \left(\frac{k}{a_1 H_1} \right)^{4-2\gamma-2\delta} F_E(k\tau, \delta), \\ F_E(x, \delta) &= \left(\frac{q}{2} \right)^{-2\delta} \left(\frac{x}{2} \right) \Gamma^2(\delta + 1/2) J_{\delta-1/2}^2(x). \end{aligned} \quad (4.21)$$

The results of Eqs. (4.20)–(4.21) only assume $x_1 < 1$ and $0 \leq \delta \ll \gamma$ and can be evaluated either for $k\tau \ll 1$ or for $k\tau \gg 1$. As long as $k\tau \ll 1$ it is enough to recall that $J_\alpha(z) \simeq (z/2)^\alpha / \Gamma(\alpha + 1)$ [42, 43]; in the opposite regime (i.e. $k\tau \gg 1$) Eq. (4.12) provides instead the valid approximation scheme¹⁸.

Another interesting limit is the sudden approximation which is not well defined a priori but only as the $\delta \rightarrow 0$ limit; in this case x and x_1 are kept fixed and the matrix elements of Eq. (4.2) assume a rather simple form implying:

$$P_B(k, \tau) = \frac{k^5}{2\pi^2} \left| \cos(x + x_1) \bar{f}_k + \sin(x + x_1) \frac{\bar{g}_k}{k} \right|^2, \quad (4.22)$$

$$P_E(k, \tau) = \frac{k^3}{2\pi^2} \left| -k \sin(x + x_1) \bar{f}_k + \cos(x + x_1) \bar{g}_k \right|^2. \quad (4.23)$$

Using Eq. (A.8) the gauge power spectra will be:

$$P_B(k, \tau) = a_1^4 H_1^4 D(\gamma + 1/2) \left(\frac{k}{a_1 H_1} \right)^{4-2\gamma} \sin^2 k\tau, \quad (4.24)$$

$$P_E(k, \tau) = a_1^4 H_1^4 D(\gamma + 1/2) \left(\frac{k}{a_1 H_1} \right)^{4-2\gamma} \cos^2 k\tau. \quad (4.25)$$

The same results of Eqs. (4.24)–(4.25) follow immediately from Eqs. (4.20)–(4.21) by recalling that $q^{-\delta} = (\delta/\gamma)^{-\delta} \rightarrow 1$ in the limit $\delta \rightarrow 0$. All in all, in the sudden approximation x_1 and x are kept fixed while $\delta \rightarrow 0$; in the smooth limit δ may be very small (i.e. $\delta \ll 1$) but it is always different from zero. These two complementary approximations commute since it can be shown that:

$$\lim_{\delta \rightarrow 0} \left[\lim_{x_1 \ll x \ll 1} \mathcal{M}(\delta, x_1, x) \right] = \lim_{x_1 \ll x \ll 1} \left[\lim_{\delta \rightarrow 0} \mathcal{M}(\delta, x_1, x) \right] = \begin{pmatrix} 1 & x \\ -x & 1 \end{pmatrix}. \quad (4.26)$$

4.2 Decreasing gauge coupling

4.2.1 Matrix for the $(\tilde{\gamma}, \tilde{\delta})$ transition

When the gauge coupling decreases and the dynamics of the transition follows the timeline of Fig. 2 the analog of Eq. (4.1) can be written as:

$$\begin{pmatrix} f_k(\tau) \\ g_k(\tau)/k \end{pmatrix} = \begin{pmatrix} \widetilde{A}_{ff}(k, \tau, \tau_1) & \widetilde{A}_{fg}(k, \tau, \tau_1) \\ \widetilde{A}_{gf}(k, \tau, \tau_1) & \widetilde{A}_{gg}(k, \tau, \tau_1) \end{pmatrix} \begin{pmatrix} \bar{f}_k \\ \bar{g}_k/k \end{pmatrix}, \quad (4.27)$$

where, as usual, $\bar{f}_k = f_k(-\tau_1)$ and $\bar{g}_k = g_k(-\tau_1)$ follow from Eq. (3.22) and their explicit expression can be found in Eq. (B.9). As usual we also added a tilde on top of the various matrix elements to stress that they are computed in the framework of the $(\tilde{\gamma}, \tilde{\delta})$ transition. Thanks to the Wronskian normalization (2.21) the analog of Eq. (4.3) is now:

$$\widetilde{A}_{ff}(k, \tau, \tau_1) \widetilde{A}_{gg}(k, \tau, \tau_1) - \widetilde{A}_{fg}(k, \tau, \tau_1) \widetilde{A}_{gf}(k, \tau, \tau_1) = 1. \quad (4.28)$$

¹⁸Equations (4.20) and (4.21) hold for any value of $k\tau$; however, as we shall argue in section 5, for $\tau > \tau_k \sim 1/k$ the power spectra will be modified by the finite value of the conductivity.

The various entries of the transition matrix appearing in Eq. (4.27) are:

$$\begin{aligned}
\widetilde{A}_{ff}(k, \tau, \tau_1) &= \frac{\pi}{2} \sqrt{qx_1} \sqrt{ky} \left[Y_{\widetilde{\nu}-1}(qx_1) J_{\widetilde{\nu}}(ky) - J_{\widetilde{\nu}-1}(qx_1) Y_{\widetilde{\nu}}(ky) \right], \\
\widetilde{A}_{fg}(k, \tau, \tau_1) &= \frac{\pi}{2} \sqrt{qx_1} \sqrt{ky} \left[J_{\widetilde{\nu}}(qx_1) Y_{\widetilde{\nu}}(ky) - Y_{\widetilde{\nu}}(qx_1) J_{\widetilde{\nu}}(ky) \right], \\
\widetilde{A}_{gf}(k, \tau, \tau_1) &= \frac{\pi}{2} \sqrt{qx_1} \sqrt{ky} \left[Y_{\widetilde{\nu}-1}(qx_1) J_{\widetilde{\nu}-1}(ky) - J_{\widetilde{\nu}-1}(qx_1) Y_{\widetilde{\nu}-1}(ky) \right], \\
\widetilde{A}_{gg}(k, \tau, \tau_1) &= \frac{\pi}{2} \sqrt{qx_1} \sqrt{ky} \left[J_{\widetilde{\nu}}(qx_1) Y_{\widetilde{\nu}-1}(ky) - Y_{\widetilde{\nu}}(qx_1) J_{\widetilde{\nu}-1}(ky) \right].
\end{aligned} \tag{4.29}$$

The matrix elements of Eq. (4.29) and the values of \bar{f}_k and \bar{g}_k are determined from the continuity of the mode functions as described in appendix B. The variables y , q and $\widetilde{\nu}$ are now functions of $\widetilde{\delta}$ and $\widetilde{\gamma}$ in full analogy with Eq. (4.4):

$$q(\widetilde{\delta}, \widetilde{\gamma}) = \frac{\widetilde{\delta}}{\widetilde{\gamma}}, \quad y(\tau, \widetilde{\delta}, \widetilde{\gamma}) = \tau + \tau_1 \left[1 + q(\widetilde{\delta}, \widetilde{\gamma}) \right], \quad \widetilde{\nu}(\widetilde{\delta}) = |\widetilde{\delta} - 1/2|. \tag{4.30}$$

Note that Eq. (4.29) has the same form of Eq. (4.2); formally Eq. (4.29) can be obtained from Eq. (4.2) by replacing ν with $\widetilde{\nu}$. With the same notations of Eq(4.6) we can define the matrix

$$\widetilde{\mathcal{M}}(\widetilde{\delta}, x, x_1) = \begin{pmatrix} \widetilde{A}_{ff}(\widetilde{\delta}, x, x_1) & \widetilde{A}_{fg}(\widetilde{\delta}, x, x_1) \\ \widetilde{A}_{gf}(\widetilde{\delta}, x, x_1) & \widetilde{A}_{gg}(\widetilde{\delta}, x, x_1) \end{pmatrix}. \tag{4.31}$$

Inserting the expressions of Eqs. (4.27) into Eqs. (2.25)–(2.26) the comoving power spectra for the $(\widetilde{\gamma}, \widetilde{\delta})$ transition are:

$$\widetilde{P}_B(k, \tau) = \frac{k^5}{2\pi^2} \left| \widetilde{A}_{ff} \bar{f}_k + \widetilde{A}_{fg} \frac{\bar{g}_k}{k} \right|^2, \tag{4.32}$$

$$\widetilde{P}_E(k, \tau) = \frac{k^3}{2\pi^2} \left| k \widetilde{A}_{gf} \bar{f}_k + \widetilde{A}_{gg} \bar{g}_k \right|^2. \tag{4.33}$$

As already argued for the (γ, δ) transition, the terms appearing inside the squared moduli at the right hand side of Eqs. (4.32) and (4.33) are not of the same order but one of the two terms will be alternatively dominant. Owing to the specific form of Eqs. (4.31) and (4.29)–(B.9) the hierarchies between the different terms contributing to Eqs. (4.32)–(4.33) turn out to be:

$$|\widetilde{A}_{ff}(\widetilde{\delta}, x, x_1) \bar{f}_k| \gg \left| \widetilde{A}_{fg}(\widetilde{\delta}, x, x_1) \frac{\bar{g}_k}{k} \right|, \tag{4.34}$$

$$|\widetilde{A}_{gf}(\widetilde{\delta}, x, x_1) \bar{f}_k| \gg \left| \widetilde{A}_{gg}(\widetilde{\delta}, x, x_1) \frac{\bar{g}_k}{k} \right|. \tag{4.35}$$

The inequalities Eqs. (4.34) and (4.35) imply that the late-time hypermagnetic power spectra are determined by the hypermagnetic power spectra at τ_1 and they can be explicitly verified by following the same strategy illustrated in the case of the (γ, δ) transition. So for instance we can rewrite Eq. (4.34) as:

$$\left| Y_{\widetilde{\nu}-1}(qx_1) J_{\widetilde{\nu}}(ky) - J_{\widetilde{\nu}-1}(qx_1) Y_{\widetilde{\nu}}(ky) \right| \gg \left| \frac{H_{\mu-1}^{(1)}(x_1)}{H_{\mu}^{(1)}(x_1)} \right| \left| J_{\widetilde{\nu}}(qx_1) Y_{\widetilde{\nu}}(ky) - Y_{\widetilde{\nu}}(qx_1) J_{\widetilde{\nu}}(ky) \right|. \tag{4.36}$$

If both sides of Eq. (4.36) are expanded for $x_1 \ll x < 1$ and with the subsidiary condition $0 \leq \widetilde{\delta} \ll \widetilde{\gamma}$ we obtain the following condition:

$$\left(\frac{qx_1}{2} \right)^{2\widetilde{\delta}} \gg \frac{\Gamma(3/2 + \widetilde{\delta}) \Gamma(|\widetilde{\gamma} - 1/2|)}{\Gamma(1/2 - \widetilde{\delta}) \Gamma(\widetilde{\gamma} + 1/2)} \left(\frac{x_1}{2} \right)^{\widetilde{\gamma} + 1/2 - |\widetilde{\gamma} - 1/2|}. \tag{4.37}$$

When $\tilde{\gamma} > 1/2$ Eq. (4.37) implies $x_1^{2\tilde{\delta}} > x_1$: this requirement is always verified for $x_1 < 1$ since, by assumption, $0 \leq \tilde{\delta} \ll 1/2$. Similarly, in the range $\tilde{\gamma} < 1/2$, Eq. (4.37) demands $x_1^{2\tilde{\delta}} > x_1^{2\tilde{\gamma}}$ which is also true since $\tilde{\delta} \ll \tilde{\gamma}$. The same logic can be applied to Eq. (4.35) but this discussion will be omitted for the sake of conciseness. All in all Eqs. (4.34) and (4.35) imply that the comoving power spectra become

$$\tilde{P}_B(k, \tau) = \frac{k^5}{2\pi^2} \left| \tilde{A}_{ff}(\tilde{\delta}, x_1, x) \tilde{f}_k \right|^2, \quad \tilde{P}_E(k, \tau) = \frac{k^3}{2\pi^2} \left| \tilde{A}_{gf}(\tilde{\delta}, x_1, x) k \tilde{f}_k \right|^2. \quad (4.38)$$

4.2.2 Explicit forms of the power spectra in various limits

The spectra of Eq. (4.38) can be evaluated in various limits and, for this purpose, it is useful to expand Eq. (4.29) for x_1 with the subsidiary conditions $0 \leq \delta < 1/2$. The result of this stem can be expressed as:

$$\tilde{A}_{ff}(\tilde{\delta}, x_1, x) = \left(\frac{qx_1}{2} \right)^{-\tilde{\delta}} \left[\sqrt{\frac{x}{2}} \Gamma(1/2 + \tilde{\delta}) J_{\tilde{\delta}-1/2}(x) + \mathcal{O}(x_1) \right] + \mathcal{O}[(qx_1)^{1+\tilde{\delta}}], \quad (4.39)$$

$$\tilde{A}_{fg}(\tilde{\delta}, x_1, x) = \left(\frac{qx_1}{2} \right)^{\tilde{\delta}} \left[\sqrt{\frac{x}{2}} \Gamma(1/2 - \tilde{\delta}) J_{-\tilde{\delta}+1/2}(x) + \mathcal{O}(x_1) \right] + \mathcal{O}[(qx_1)^{1-\tilde{\delta}}], \quad (4.40)$$

$$\tilde{A}_{gf}(\tilde{\delta}, x_1, x) = \left(\frac{qx_1}{2} \right)^{-\tilde{\delta}} \left[-\sqrt{\frac{x}{2}} \Gamma(1/2 + \tilde{\delta}) J_{1/2+\tilde{\delta}}(x) + \mathcal{O}(x_1) \right] + \mathcal{O}[(qx_1)^{1+\tilde{\delta}}], \quad (4.41)$$

$$\tilde{A}_{gg}(\tilde{\delta}, x_1, x) = \left(\frac{qx_1}{2} \right)^{\tilde{\delta}} \left[\sqrt{\frac{x}{2}} \Gamma(1/2 - \tilde{\delta}) J_{-\tilde{\delta}-1/2}(x) + \mathcal{O}(x_1) \right] + \mathcal{O}[(qx_1)^{1-\tilde{\delta}}]. \quad (4.42)$$

Again using Eqs. (4.39)–(4.40) and (4.41)–(4.42) the inequalities (4.34)–(4.35) are verified and the corresponding power spectra turn out to be:

$$\begin{aligned} \tilde{P}_B(k, \tau) &= a_1^4 H_1^4 D(\tilde{\gamma} + 1/2) \left(\frac{k}{a_1 H_1} \right)^{4-2\tilde{\gamma}-2\tilde{\delta}} \tilde{F}_B(k\tau, \tilde{\delta}), \\ \tilde{F}_B(x, \tilde{\delta}) &= \left(\frac{q}{2} \right)^{-2\tilde{\delta}} \left(\frac{x}{2} \right) \Gamma^2(\delta + 1/2) J_{\delta-1/2}^2(x). \end{aligned} \quad (4.43)$$

From Eq. (4.15) and (4.19) the hyperelectric spectrum is

$$\begin{aligned} \tilde{P}_E(k, \tau) &= a_1^4 H_1^4 D(\tilde{\gamma} + 1/2) \left(\frac{k}{a_1 H_1} \right)^{4-2\tilde{\gamma}-2\tilde{\delta}} \tilde{F}_E(k\tau, \tilde{\delta}), \\ \tilde{F}_E(x, \tilde{\delta}) &= \left(\frac{q}{2} \right)^{-2\tilde{\delta}} \left(\frac{x}{2} \right) \Gamma^2(\tilde{\delta} + 1/2) J_{\tilde{\delta}+1/2}^2(x). \end{aligned} \quad (4.44)$$

Equations (4.43) and (4.44) can be evaluated in the sudden approximation by taking the limit $\tilde{\delta} \rightarrow 0$ while x and x_1 are kept fixed; the gauge power spectra are, in this case¹⁹

$$\tilde{P}_B(k, \tau) = a_1^4 H_1^4 D(\tilde{\gamma} + 1/2) \left(\frac{k}{a_1 H_1} \right)^{4-2\tilde{\gamma}} \cos^2 k\tau, \quad (4.45)$$

$$\tilde{P}_E(k, \tau) = a_1^4 H_1^4 D(\tilde{\gamma} + 1/2) \left(\frac{k}{a_1 H_1} \right)^{4-2\tilde{\gamma}} \sin^2 k\tau. \quad (4.46)$$

By comparing Eqs. (4.45)–(4.46) with the analog results given in Eqs. (4.24)–(4.25) we note that the phases of the Sakharov oscillations are exchanged: while $P_B(k, \tau)$ oscillates like $\sin^2 k\tau$, the oscillations of $\tilde{P}_B(k, \tau)$ go like $\cos^2 k\tau$. The opposite is true for the hyperelectric power spectra. The differences in the phases of oscillation are a particular consequence of duality which will now be analyzed in general terms.

¹⁹Note that the same results of Eqs. (4.45)–(4.46) follow immediately from Eqs. (4.43)–(4.44) by recalling that $q^{-\tilde{\delta}} = (\tilde{\delta}/\tilde{\gamma})^{-\tilde{\delta}} \rightarrow 1$ in the limit $\tilde{\delta} \rightarrow 0$.

4.3 Duality and continuity of the power spectra after inflation

During inflation duality relates the gauge power spectra in different dynamical situations (see Eqs. (3.32)–(3.33)). When the gauge coupling flattens out the gauge power spectra are also related by duality which is equivalent to the following transformation:

$$(\gamma, \delta) \rightarrow (\tilde{\gamma}, \tilde{\delta}). \quad (4.47)$$

The action of Eq. (4.47) transforms the elements of the transition matrix according to

$$A_{ff} \rightarrow \tilde{A}_{gg}, \quad A_{gg} \rightarrow \tilde{A}_{ff}, \quad A_{fg} \rightarrow -\tilde{A}_{gf}, \quad A_{gf} \rightarrow -\tilde{A}_{fg}. \quad (4.48)$$

Equation (4.48) follows from the expressions of the matrix elements reported in Eqs. (4.2) and (4.29). For the sake of accuracy the results of Eq. (4.48) have been explicitly derived in appendix C. Moreover \bar{f}_k and \bar{g}_k will transform under duality as $\bar{f}_k \rightarrow \bar{g}_k/k$ and $\bar{g}_k \rightarrow -k \bar{f}_k$. Thanks to Eqs. (2.29) and (4.48) the action of Eq. (4.47) transforms the gauge power spectra as:

$$P_B(k, \tau) \rightarrow \tilde{P}_E(k, \tau), \quad P_E(k, \tau) \rightarrow \tilde{P}_B(k, \tau). \quad (4.49)$$

Also the approximate expressions of the power spectra, if they are correct, must transform according to Eq. (4.49) since they must be consistent with duality; in particular:

- the approximate power spectrum $P_B(k, \tau)$ of Eq. (4.20) gives the approximate form of \tilde{P}_E (i.e. Eq. (4.44));
- the transformation (4.47) applied to Eq. (4.21) gives the approximate form of the hypermagnetic power spectrum in the dual description (i.e. $P_E(k, \tau) \rightarrow \tilde{P}_B(k, \tau)$);
- in the sudden approximation (when $\delta \rightarrow 0$ and $\tilde{\delta} \rightarrow 0$) the gauge power spectra of Eqs. (4.7)–(4.8) and (4.32)–(4.33) are related by duality

All in all during inflation duality implies that when the gauge coupling increases the magnetic spectrum is never flat and if the gauge coupling is instead decreasing the electric spectrum is never flat. After inflation duality constrains the explicit forms of the gauge power spectra and the phases of the Sakharov oscillations. If the gauge coupling flattens out after a phase of increasing coupling the late-time gauge spectra are determined by the hyperelectric spectrum at the end of inflation. In the dual situation the gauge coupling freezes after a stage of decreasing coupling. Barring for the possible physical justifications of a strongly coupled phase at the beginning of inflation, the late-time gauge power spectra follow from the hypermagnetic spectrum at the end of inflation.

5 Phenomenological considerations

The hypercharge field projects on the electromagnetic fields through the cosine of the Weinberg angle (i.e. $\cos \theta_W$) so that the late-time gauge power spectra could be compared both with the magnetogenesis requirements and with other phenomenological constraints. In this section we adopt the standard notations commonly employed in the context of the concordance paradigm. So for instance Ω_{R0} denotes present critical fraction of relativistic particles, Ω_{M0} is total critical fraction of massive species, r_T defines the ratio between the tensor and scalar power spectra at the pivot scale $k_p = 0.002 \text{ Mpc}^{-1}$ and so on and so forth. The present value of the scale factor will be normalized to 1 (i.e. $a_0 = 1$) and, thanks to this widely used convention, the physical and the comoving frequencies coincide at the present time. The present section is devoted to phenomenological implications; in particular the following topics will be specifically treated;

- in subsection 5.1 a brief summary of the typical scales of the problem has been provided in a phenomenological perspective;
- in subsection 5.2 some simplified estimates of the physical spectra before reentry have been discussed;
- subsection 5.3 is devoted to the physical spectra after reentry;
- in subsection 5.4 we give a specific discussion of the magnetogenesis constraints in a self-contained perspective;
- the dependence the parameter space of the model has been charted in the subsection 5.5;
- the subsection 5.6 has been devoted to the effects of a post-inflationary phase preceding the radiation epoch;
- a final assessment of the obtained results has been presented in the subsection 5.7.

5.1 Scales of the problem

Defining with $\tau_k = 1/k$ the reentry time of a generic wavelength, the ratio between τ_k and the time of matter-radiation equality τ_{eq} is:

$$\frac{\tau_k}{\tau_{eq}} = 1.06 \times 10^{-2} \left(\frac{h_0^2 \Omega_{M0}}{0.1386} \right) \left(\frac{h_0^2 \Omega_{R0}}{4.15 \times 10^{-5}} \right)^{-1/2} \left(\frac{k}{\text{Mpc}^{-1}} \right)^{-1}, \quad (5.1)$$

since $(\tau_k/\tau_{eq}) = \sqrt{2}(H_0/k)\Omega_{M0}/\sqrt{\Omega_{R0}}$ and $H_0 = 100 h_0 \text{ (km/Mpc) Hz}$ denotes the present value of the Hubble rate. Consequently the relevant wavenumbers for magnetogenesis considerations [i.e. $k = \mathcal{O}(\text{Mpc}^{-1})$] reentered prior to matter radiation equality.

After the gauge coupling flattens out the amplitude of the comoving power spectra is $\mathcal{O}(H_1^4)$ (see, for instance, Eqs. (4.20)–(4.21) and (4.43)–(4.44)). The inflationary Hubble rate H_1 is related to the Planck scale as²⁰:

$$\frac{H_1}{M_P} = \sqrt{\pi \epsilon \mathcal{A}_R} = 2.17 \times 10^{-6} \left(\frac{r_T}{0.01} \right)^{1/2} \left(\frac{\mathcal{A}_R}{2.41 \times 10^{-9}} \right)^{1/2}, \quad (5.2)$$

where \mathcal{A}_R denotes the amplitude of the scalar power spectrum at the pivot scale $k_p = 0.002 \text{ Mpc}^{-1}$. Thanks to Eq. (5.2) it is then possible to express H_1^4 in units of nG^2 by recalling that $M_P^4 = 4.62 \times 10^{132} \text{ nG}^2$. The scale H_1 also enters the explicit expression of $x_1 = k\tau_1 = k/(a_1 H_1)$:

$$\frac{k}{a_1 H_1} = \frac{k}{a_0 H_0} \left(\frac{a_0 H_0}{a_1 H_1} \right) = \frac{k}{H_0} \zeta_r^{1/2-\alpha} \left(2\pi \epsilon \Omega_{R0} \mathcal{A}_R \right)^{-1/4} \sqrt{\frac{H_0}{M_P}}, \quad (5.3)$$

where the first equality is just true by definition while the second one is the explicit estimate. As already mentioned, in Eq. (5.3) Ω_{R0} is the (present) critical fraction of massless species (in the concordance paradigm $h_0^2 \Omega_{R0} = 4.15 \times 10^{-5}$); note that H_0 is usefully expressed in Planck units as $(H_0/M_P) = 1.22 \times 10^{-61} (h_0/0.7)$. In terms of the typical values of the various parameters, Eq. (5.3) can also be written in the following revealing form:

$$\frac{k}{a_1 H_1} = 10^{-23.05} \left(\frac{k}{\text{Mpc}^{-1}} \right) \left(\frac{r_T}{0.01} \right)^{-1/4} \left(\frac{h_0^2 \Omega_{R0}}{4.15 \times 10^{-5}} \right)^{-1/4} \left(\frac{\mathcal{A}_R}{2.41 \times 10^{-9}} \right)^{-1/4} \zeta_r^{1/2-\alpha}. \quad (5.4)$$

In Eqs. (5.3)–(5.4) $\zeta_r = H_r/H_1$ and H_r is the value of the Hubble rate at the moment when the radiation starts dominating; in the concordance paradigm $\zeta_r = 1$ (and this is the value we shall assume most of

²⁰In Eq. (5.2) we traded ϵ for the tensor scalar ratio r_T by using the consistency relation $r_T = 16 \epsilon$.

the time). However it is sometimes useful to check for the stability of the obtained results with respect to a change of the reference scenario. This is why Eqs. (5.3)–(5.4) have been derived by considering a generalized post-inflationary evolution where the radiation epoch is preceded by a phase expanding at a rate parametrized²¹ by α . Finally, throughout the explicit numerical evaluation it will be useful to bear in mind the following two general expressions:

$$\left(\frac{a_1}{a_0}\right) = \zeta_r^{\alpha-1/2} \left(\frac{2\Omega_{R0}}{\pi\epsilon\mathcal{A}_{\mathcal{R}}}\right)^{1/4} \sqrt{\frac{H_0}{M_P}}, \quad \left(\frac{a_0 H_0}{a_1 H_1}\right) = \zeta_r^{1/2-\alpha} \left(2\pi\epsilon\Omega_{R0}\mathcal{A}_{\mathcal{R}}\right)^{-1/4} \sqrt{\frac{H_0}{M_P}}. \quad (5.5)$$

5.2 Physical spectra prior to reentry

In the previous sections we discussed mainly the comoving spectra of the hyperelectric and hypermagnetic fields but in various situations the distinction between the physical and the comoving fields has played a crucial role. The distinction between physical and comoving power spectra has been given in Eq. (2.27) and here we just want to illustrate, in a preliminary respective, the evolution of the comoving fields as a function of $k\tau$. In Fig. 3 we illustrate the evolution of the common logarithm of the square roots of the

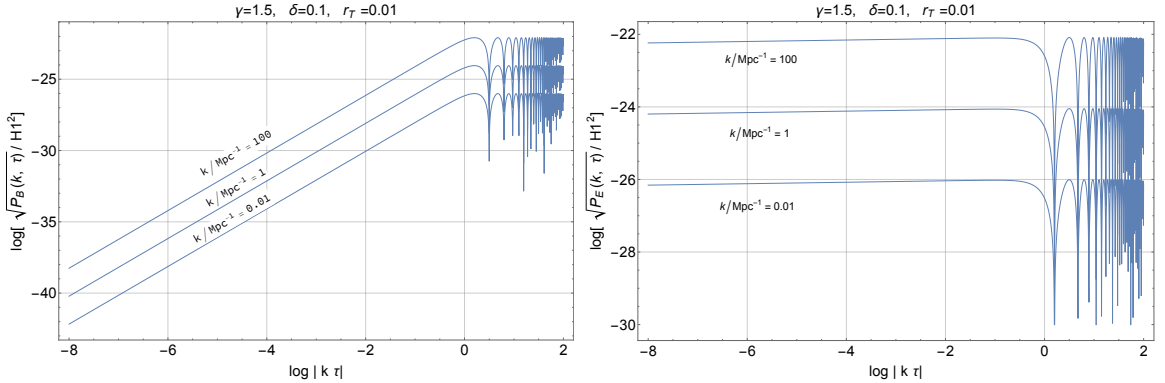


Figure 3: We illustrate the comoving power spectra prior to reentry for a particular choice of the parameters and for three different comoving scales.

hyperelectric and hypermagnetic power spectra²² as a function of the common logarithm of $|k\tau|$. The values of γ and δ have been randomly chosen since the parameter space will be more carefully scrutinised in subsection 5.5. In Fig. 3 three different scales have been included. The most relevant one is the scale of the primordial gravitational collapse (i.e. $k = \mathcal{O}(\text{Mpc}^{-1})$). The other two scales are just illustrative but the same bunch of wavenumbers will be illustrated in the contour plots of subsection 5.5.

For $\tau \ll \tau_k$ the power spectra follow from Eqs. (4.20)–(4.21) and (4.43)–(4.44) evaluated in the limit $k\tau \ll 1$. When the gauge coupling increases the physical spectra (2.27) associated with the comoving expressions of Eqs. (4.20)–(4.21) are²³:

$$P_B^{(phys)}(k, \tau) = \frac{H_1^4}{\lambda_1} \left(\frac{a_1}{a}\right)^4 \frac{D(\gamma+1/2)}{(2\delta+1)^2 q^{4\delta}} \left(\frac{k}{a_1 H_1}\right)^{6-2\gamma} \left(\frac{a_1 H_1}{a H}\right)^{4\delta+2}, \quad (5.6)$$

$$P_E^{(phys)}(k, \tau) = \frac{H_1^4}{\lambda_1} \left(\frac{a_1}{a}\right)^4 \frac{D(\gamma+1/2)}{q^{4\delta}} \left(\frac{k}{a_1 H_1}\right)^{4-2\gamma} \left(\frac{a_1 H_1}{a H}\right)^{4\delta}, \quad \tau < \tau_k. \quad (5.7)$$

²¹If this intermediate stage of expansion is dominated by a perfect fluid with barotropic index w , we have that $\alpha = 2/[3(w+1)]$.

²²The electromagnetic projection of the hypercharge through the Weinberg angle has not been included but it will be carefully taken into account when charting the parameter space in subsection 5.5.

²³Concerning Eqs. (5.6) and (5.7) we note that $\lambda_1 = \lambda(-\tau_1)$. For the sake of simplicity we shall assume $\lambda_1 = 1$ even if λ_1 could also be slightly larger than 1.

When the gauge coupling decreases the comoving spectra of Eqs. (4.43)–(4.44) must be inserted into Eq. (2.27) and the result is:

$$\widetilde{P}_B^{(phys)}(k, \tau) = \frac{H_1^4}{\lambda_1} \left(\frac{a_1}{a}\right)^4 \frac{D(\tilde{\gamma} + 1/2)}{q^{4\tilde{\delta}}} \left(\frac{k}{a_1 H_1}\right)^{4-2\tilde{\gamma}} \left(\frac{a_1 H_1}{a H}\right)^{4\tilde{\delta}}, \quad (5.8)$$

$$\widetilde{P}_E^{(phys)}(k, \tau) = \frac{H_1^4}{\lambda_1} \left(\frac{a_1}{a}\right)^4 \frac{D(\tilde{\gamma} + 1/2)}{(2\tilde{\delta} + 1)^2 q^{4\tilde{\delta}}} \left(\frac{k}{a_1 H_1}\right)^{6-2\tilde{\gamma}} \left(\frac{a_1 H_1}{a H}\right)^{4\tilde{\delta}+2}, \quad \tau < \tau_k. \quad (5.9)$$

The explicit formulas of Eqs. (5.2)–(5.3) and (5.5) allow for an explicit evaluation of Eqs. (5.6)–(5.7) and (5.8)–(5.9). If $\lambda_1 = \mathcal{O}(1)$ the only spectra consistent with the perturbative evolution of the gauge coupling are the ones of Eqs. (5.6)–(5.7). In the case of decreasing gauge coupling λ_1 must be instead extremely large (see also Eq. (2.44) and discussion therein). This means, however, that the magnetic spectrum (5.8) will be suppressed as $\lambda_1^{-1} \simeq e^{-2\tilde{\gamma}N}$ where N now denotes the total number of inflationary e -folds. Let us finally remark that in the sudden limit (i.e. $\delta \rightarrow 0$ and $\tilde{\delta} \rightarrow 0$) the physical power spectra will always follow from Eq. (2.27) but the related comoving spectra will be given, respectively, by Eqs. (4.24)–(4.25) and (4.45)–(4.46). For instance, in the case of increasing gauge coupling the result will be:

$$P_B^{(phys)}(k, \tau) = \frac{H_1^4}{\lambda_1} \left(\frac{a_1}{a}\right)^4 D(\gamma + 1/2) \left(\frac{k}{a_1 H_1}\right)^{6-2\gamma} \left(\frac{a_1 H_1}{a H}\right)^2, \quad (5.10)$$

$$P_E^{(phys)}(k, \tau) = \frac{H_1^4}{\lambda_1} \left(\frac{a_1}{a}\right)^4 D(\gamma + 1/2) \left(\frac{k}{a_1 H_1}\right)^{4-2\gamma}, \quad \tau < \tau_k. \quad (5.11)$$

5.3 Physical spectra after reentry

For $\tau \geq \tau_k$ the evolution of the mode functions is modified by the presence of the conductivity and it is approximately given by²⁴:

$$g'_k = -k^2 f_k - \sigma g_k, \quad f'_k = g_k. \quad (5.12)$$

These equations can be systematically solved as an expansion in (k/σ) by setting initial conditions at $\tau = \tau_k$. To lowest order the solution of Eq. (5.12) for $\tau \geq \tau_k$ is:

$$f_k(\tau) = A_g f(k, \tau_1, \tau_k) \frac{\bar{g}_k}{k} e^{-\frac{k^2}{k_\sigma^2}}, \quad g_k(\tau) = \left(\frac{k}{\sigma}\right) A_g g(k, \tau_1, \tau_k) \bar{g}_k e^{-\frac{k^2}{k_\sigma^2}}, \quad (5.13)$$

where the magnetic diffusivity scale k_σ has been defined as $k_\sigma^{-2} = \int_{\tau_k}^{\tau} dz/\sigma(z)$. While the estimate of k_σ can be made accurate by computing the transport coefficients of the plasma in different regimes, for the present purposes this is not necessary since the ratio $(k/k_\sigma)^2$ is so small, for the phenomenologically interesting scales, that the negative exponentials in Eq. (5.13) evaluate to 1. In fact by taking $\tau = \tau_{\text{eq}}$ we have that k_σ can be estimated as:

$$\left(\frac{k}{k_\sigma}\right)^2 = \frac{4.75 \times 10^{-26}}{\sqrt{2 h_0^2 \Omega_{M0}(z_{\text{eq}} + 1)}} \left(\frac{k}{\text{Mpc}^{-1}}\right)^2, \quad (5.14)$$

where Ω_{M0} is the present critical fraction in matter and $z_{\text{eq}} + 1 = a_0/a_{\text{eq}} \simeq \mathcal{O}(3200)$ is the redshift of matter-radiation equality. The physical power spectra after for $\tau \gg \tau_k$ will then be given by:

$$P_B^{(phys)}(k, \tau) = H_1^4 \left(\frac{a_1}{a}\right)^4 D(\gamma + 1/2) \left(\frac{k}{a_1 H_1}\right)^{4-2\gamma-2\delta} F_B(k\tau_k, \delta) e^{-2\frac{k^2}{k_\sigma^2}}, \quad (5.15)$$

$$P_E^{(phys)}(k, \tau) = \left(\frac{k}{\sigma}\right)^2 H_1^4 \left(\frac{a_1}{a}\right)^4 D(\gamma + 1/2) \left(\frac{k}{a_1 H_1}\right)^{4-2\gamma-2\delta} F_E(k\tau_k, \delta) e^{-2\frac{k^2}{k_\sigma^2}}. \quad (5.16)$$

²⁴Note that in a different system of units (where the gauge coupling is defined without the $\sqrt{4\pi}$ factor) we would have $4\pi\sigma$ (and not simply σ) in Eq. (5.12). We are assuming here that the gauge coupling does not evolve anymore and it is frozen to its constant value.

where $F_B(x, \delta)$ and $F_E(x, \delta)$ coincide with the ones defined in Eqs. (4.20)–(4.21).

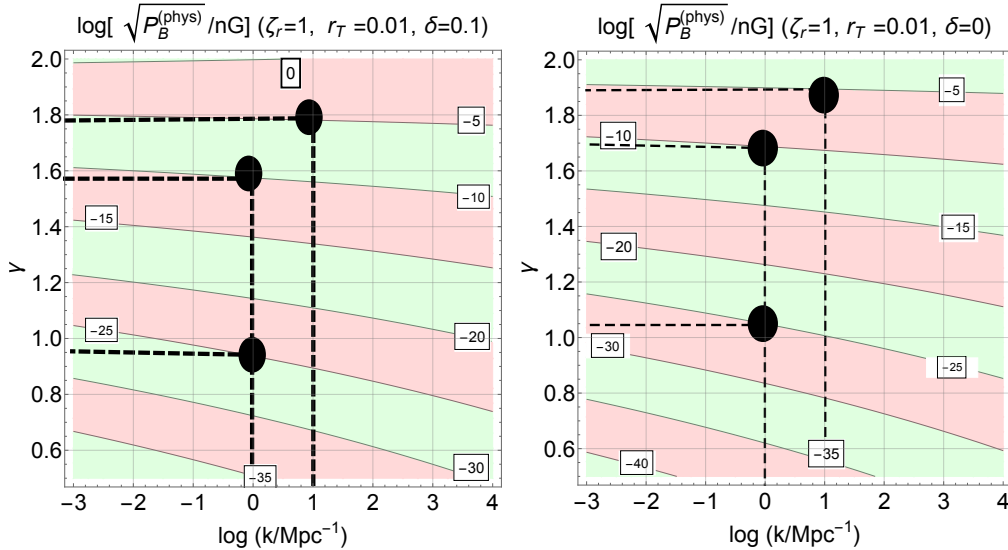


Figure 4: The parameter space is illustrated in the (γ, k) plane. The numbers appearing on the various contours correspond to the common logarithm of the physical power spectrum. The common logarithm of k in units of Mpc^{-1} is reported on the horizontal axis.

According to Eqs. (5.15)–(5.16) the magnetic spectrum for $k < k_\sigma$ is practically not affected by the conductivity while the electric power spectrum is suppressed by $k^2/\sigma^2 \ll 1$. Since prior to decoupling the electron-photon and electron-proton interactions tie the temperatures close together, the conductivity scales as $\sigma \sim \sqrt{T/m_e T}/\alpha_{em}$ where m_e is the electromagnetic mass, T is the temperature and α_{em} is the fine structure constant. For instance, if we take $T = \mathcal{O}(\text{eV})$ we get $k/\sigma = \mathcal{O}(10^{-30})$ for $k = \mathcal{O}(\text{Mpc}^{-1})$. The electric power spectrum of Eq. (5.16) will then be suppressed, in comparison with the magnetic spectrum, by a factor ranging between 40 and 60 orders of magnitude. This also demonstrates, in practical terms, that the duality symmetry is broken for $\tau > \tau_k$.

5.4 Magnetogenesis constraints

According to the standard lore the observed large-scale fields in galaxies (and to some extent in clusters) should have been much smaller before the gravitational collapse of the protogalaxy. Compressional amplification typically increases the initial values of the magnetic seeds by 4 or even 5 orders of magnitude and the logic underlying this statement is in short the following (see e. g. [19, 20, 21]). When the protogalactic matter collapsed by gravitational instability over a typical scale $\mathcal{O}(\text{Mpc})$ the mean matter density before collapse was of the order of ρ_{crit} , whereas right after the collapse the mean matter density became, approximately, six orders of magnitude larger than the critical density. Since the physical size of the patch decreases from 1 Mpc to 30 kpc the magnetic field increases, because of flux conservation, of a factor $(\rho_a/\rho_b)^{2/3} \sim 10^4$ where ρ_a and ρ_b are, respectively the energy densities right after and right before gravitational collapse. Most of the work in the context of the dynamo theory focuses on reproducing the correct features of the magnetic field of our galaxy. The dynamo term may be responsible for the origin of the magnetic field of the galaxy. The galaxy has a typical rotation period of 3×10^8 yrs and comparing this figure with the typical age of the galaxy, $\mathcal{O}(10^{10}\text{yrs})$, it can be appreciated that the galaxy performed about 30 rotations since the time of the protogalactic collapse. The achievable amplification produced by the dynamo instability can be at most of 10^{13} , i.e. e^{30} . Thus, if the present value of the galactic magnetic field is $\mathcal{O}(\mu\text{G})$, its value right after the gravitational collapse of the protogalaxy might have been as small as $\mathcal{O}(10^{-10})$ nG over a typical scale of 30–100 kpc.

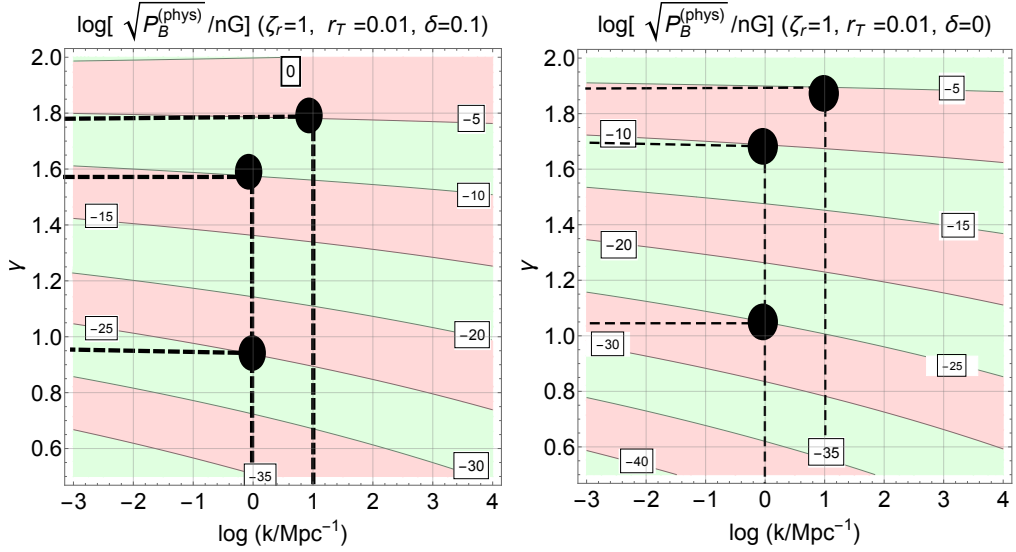


Figure 5: We illustrate the common logarithm of the power spectrum in the plane (γ, r_T) . We remind that r_T denotes, within the present notations, the tensor to scalar ratio.

	$\gamma = 1.8, \delta = 0.01$	$\gamma = 1.9, \delta = 0.01$	$\gamma = 2, \delta = 0.01$
$k = 1 \text{ Mpc}^{-1}$	$\sqrt{P_B^{(phys)}} = 10^{-7.3} \text{ nG}$	$\sqrt{P_B^{(phys)}} = 10^{-4.9} \text{ nG}$	$\sqrt{P_B^{(phys)}} = 10^{-2.30} \text{ nG}$
$k = 0.1 \text{ Mpc}^{-1}$	$\sqrt{P_B^{(phys)}} = 10^{-7.25} \text{ nG}$	$\sqrt{P_B^{(phys)}} = 10^{-4.78} \text{ nG}$	$\sqrt{P_B^{(phys)}} = 10^{-2.29} \text{ nG}$
$k = 0.01 \text{ Mpc}^{-1}$	$\sqrt{P_B^{(phys)}} = 10^{-7.44} \text{ nG}$	$\sqrt{P_B^{(phys)}} = 10^{-4.87} \text{ nG}$	$\sqrt{P_B^{(phys)}} = 10^{-2.28} \text{ nG}$

Table 1: Numerical values of the magnetic power spectrum at different scales and in the framework of the (γ, δ) transition where the gauge coupling is perturbative throughout all the stages of its evolution.

The compressional amplification and the dynamical action are typically combined together so that the magnetogenesis requirements roughly demand that the magnetic fields at the time of the gravitational collapse of the protogalaxy should be approximately larger than a (minimal) power spectrum which can be estimated between $\mathcal{O}(10^{-32}) \text{ nG}^2$ and $\mathcal{O}(10^{-22}) \text{ nG}^2$:

$$\log \left(\frac{\sqrt{P_B^{(phys)}}}{\text{nG}} \right) \geq -\xi, \quad 11 < \xi < 16. \quad (5.17)$$

The least demanding requirement of Eq. (5.17) (i.e. $\sqrt{P_B^{(phys)}} \geq 10^{-16} \text{ nG}$) follows by assuming that, after compressional amplification, every rotation of the galaxy increases the initial magnetic field of one e -fold. According to some this requirement is not completely since it takes more than one e -fold to increase the value of the magnetic field by one order of magnitude and this is the rationale for the most demanding condition of Eq. (5.17), i.e. $\sqrt{P_B^{(phys)}} \geq 10^{-11} \text{ nG}$.

5.5 Charting the parameter space

Let us now consider a simplified estimate where $\zeta_r \rightarrow 1$ and $\alpha \rightarrow 0$. This is the situation of the concordance paradigm and for the typical values of the parameters given above the results for $\sqrt{P_B^{(phys)}}(k, \tau_0)$

are reported in Tab. 1 for different values of γ and k . Since the non-screened vector modes of the hypercharge field project on the electromagnetic fields through the cosine of the Weinberg angle the estimates of Tab. 1 follow from Eq. (5.15) after multiplying the obtained result by $\cos \theta_W$ (recall, in this respect, that $\sin^2 \theta_W \simeq 0.22$). The illustrative orders of magnitude of Tab. 1 will now be complemented with more detailed estimates allowing for a simultaneous variation of the different parameters in the light of the typical figures required by the magnetogenesis considerations.

We shall distinguish the results obtained in the smooth (i.e. $\delta \ll \gamma$) and the sudden (i.e. $\delta \rightarrow 0$) approximations. In practice this will be achieved by illustrating all the subsequent numerical results for $\delta = 0.1$ and the case $\delta = 0$. In Fig. 4 the physical power spectrum is illustrated in the (k, γ) plane. The black blobs in both plots indicate three reasonable regions of the parameter space where all the pertinent phenomenological constraints are satisfied. The numbers on the various curves denote, as explained on top of the plot, the common logarithms of $\sqrt{P_B^{(phys)}}$ (expressed in nG) along that curve. By looking at the intercept on the γ axis we see that the phenomenologically reasonable values of γ correspond to spectra that are blue or, at most, quasi-flat but always slightly increasing with k (as already suggested by the results of Tab. 1).

The results of Fig. 4 are complemented by Fig. 5 where the power spectra are illustrated in the (γ, r_T) plane for fixed wavenumber $k = \text{Mpc}^{-1}$. The black blobs correspond this time to the regions where $r_T = \mathcal{O}(0.01)$: for instance in Ref. [50] the combination of different data sets implies $r_T < 0.07$ while in Ref. [51] the range of values $r_T < 0.064$ is quoted. By looking simultaneously at Figs. 4 and 5 we can appreciate that the viable range of γ roughly extends between 1.3 and 2.

5.6 Post-inflationary phases preceding the radiation epoch and reheating dynamics

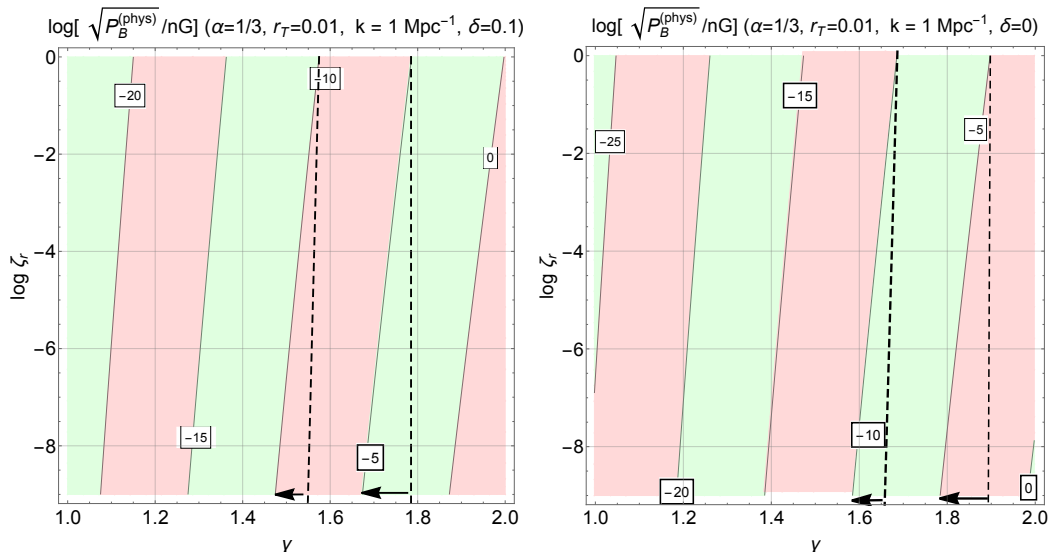


Figure 6: We illustrate the parameter space in the (γ, ζ_r) plane for a typical expansion rate $\alpha = 1/3$ corresponding to a post-inflationary stiff phase.

The results obtained so far also follow the continuity of the extrinsic curvature across the inflationary boundary. This approximation is customarily dubbed instant reheating and it is often used when setting bounds on quantities like the number of inflationary e -folds and the tensor to scalar ratio (see e.g. [50, 51]). The explosive particle decay as well as other non-perturbative effects related to the preheating dynamics probably bring the situation closer to the case of an instant reheating (see e.g. [52, 53]). However, if the reheating is perturbative as originally suggested in the new inflationary scenario [54] the effect of the

duration of the reheating phase may be relevant (see also [47]).

In Figs. 6, 7 and 8 we illustrated the situation where the dominance of radiation is *preceded* by a post-inflationary phase extending down to the relatively small values of the curvature scale. We remind from Eqs. (5.3)–(5.4) that $\zeta_r = H_r/H_1$ and H_r denotes the Hubble rate at the onset of the radiation dominance. Since α measures the expansion rate between H_1 and H_r , the parameter space of the model can also be investigated by varying α and ζ_r . For instance in Fig. 6 the value of α has been fixed (i.e. $\alpha \rightarrow 1/3$ as indicated in each of the two plots) and the contours of constant magnetic spectrum²⁵ have been investigated in the (γ, ζ_r) plane. It is now relevant to consider with care the dashed lines in Fig. 6: we see that the same amplitude of the magnetic power spectrum associated to a certain value of γ when $\zeta_r \rightarrow 1$ (i.e. in the absence of an intermediate phase) can be obtained for a comparatively *lower* value of γ if the intermediate phase is present (i.e. $\zeta_r < 1$). This is the meaning of the arrows appearing in Fig. 6: for $\alpha = 1/3$ (and for a given $\zeta_r < 1$) the γ required to obtain a certain value of the power spectrum is comparatively smaller than in the case $\zeta_r = 1$. This conclusion depends on the value of α : in Fig. 6 the case $\alpha = 1/3$ is meant to represent a post-inflationary phase dominated by a stiff fluid expanding at a rate *slower than radiation*.

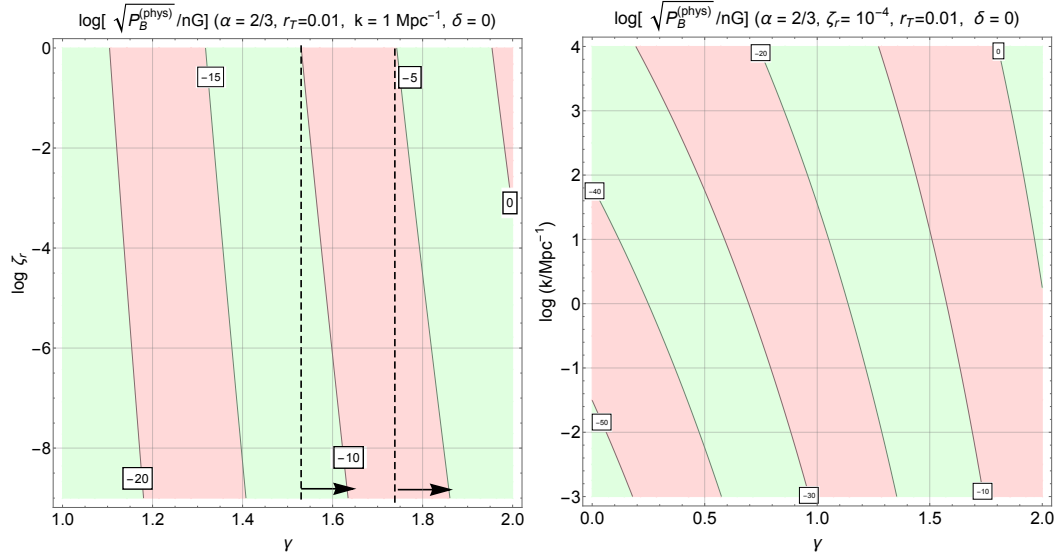


Figure 7: In the plot at the left the parameter space is illustrated in the (γ, ζ_r) plane while in the plot at the right the parameter space is instead illustrated in the (γ, k) plane. In both plots the typical expansion rate is faster than radiation (i.e. $\alpha = 2/3$) as it happens, for instance, in the context of the reheating dynamics.

In the case of an extended reheating dynamics the expansion rate prior to the dominance of radiation is expected to be faster than in the stiff case. In Fig. 7 we then considered the possibility of a post-inflationary phase preceding the ordinary radiation phase where the expansion rate is effectively faster than radiation. By looking at the dashed lines in Fig. 7 we see that the situation differs from the one illustrated in Fig. 6: for $\alpha = 2/3$ (and for a given $\zeta_r < 1$) the γ required to obtain a certain value of the power spectrum is comparatively larger than in the case $\zeta_r = 1$. The same conclusion holds for different expansion rates faster than radiation. Along this perspective we can therefore consider the plane (α, ζ_r) for a fixed value of γ (e.g. $\gamma \rightarrow 3/2$, as in Fig. 8). As ζ_r diminishes (i.e. the post-inflationary phase gets longer) the power spectrum gets *larger*. In Fig. 8 we considered the situation where the expansion rate during the intermediate phase was slower than radiation and we have also purposely chosen $\gamma = 3/2$. For larger values of γ the amplitude

²⁵We remind that the values of the magnetic power spectrum reported on each of the curves remain *the same all along the curve* since this is the meaning of a contour plot.

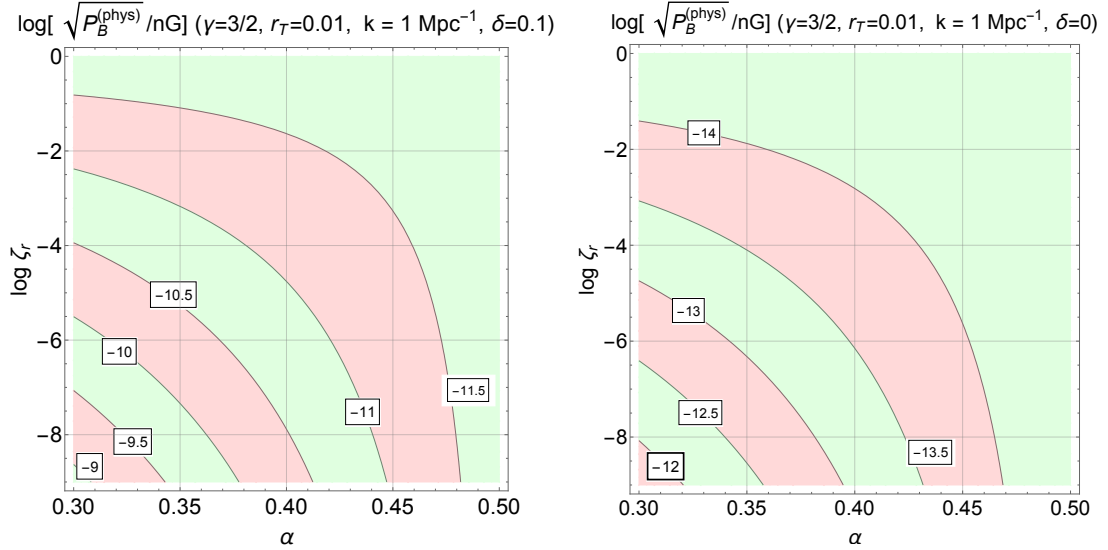


Figure 8: The allowed region of the parameter space is illustrated (α, ζ_r) plane for a fixed value of γ .

of the power spectra will be larger but the basic trend of Fig. 8 will remain the same. All in all we can therefore say that the inclusion of a post-inflationary phase preceding the ordinary radiation-dominated stage has a threefold effect depending on the expansion rate:

- if the post-inflationary phase preceding radiation expands faster than radiation the amplitude of the power spectrum gets mildly reduced for a fixed value of γ ; this means that to achieve the same amplitude we should have a comparatively larger value of γ ;
- if the post-inflationary phase expands at a rate slower than radiation (as it happens in the case of stiff post-inflationary phases) the power spectrum is mildly enhanced, i.e. to achieve the same spectral amplitude we should have a comparatively smaller value of γ ;
- in both cases the length of the post-inflationary phase is crucial: for a long stiff post-inflationary phase the amplitude of the magnetic power spectrum *gets larger*; conversely for a delayed reheating expanding faster than radiation the power spectrum gets reduced.

We finally mention that the effects of a post-inflationary phase have been qualified as *mild* in the previous list of items. By this we simply mean that for an excursion of ζ_r of about 9 orders of magnitude the spectral index gets renormalised by a factor of the order of 0.1. So this preliminary analysis seems to confirm that these are not large effects.

5.7 Final assessment of the obtained results and the meaning of the parameter space

Since this analysis has not been done before it is appropriate, as we conclude, to summarize the main results. The first aspect we stress is that has been explicitly used to deduce the gauge power spectra both during inflation and at late times. The symmetry can therefore be used to verify and constrain the explicit expressions of the power spectra.

If the gauge coupling increases during a quasi-de Sitter stage of expansion only the hyperelectric spectrum can be flat for typical wavelengths larger than the effective horizon during inflation [see e.g. Eq. (3.13) and discussions therein]. The duality symmetry implies therefore that only the hypermagnetic spectrum can be flat [see Eq. (3.28)] during a quasi-de Sitter stage of expansion and for typical wavelengths larger than the effective horizon. These results, even if not explicitly related to the duality symmetry,

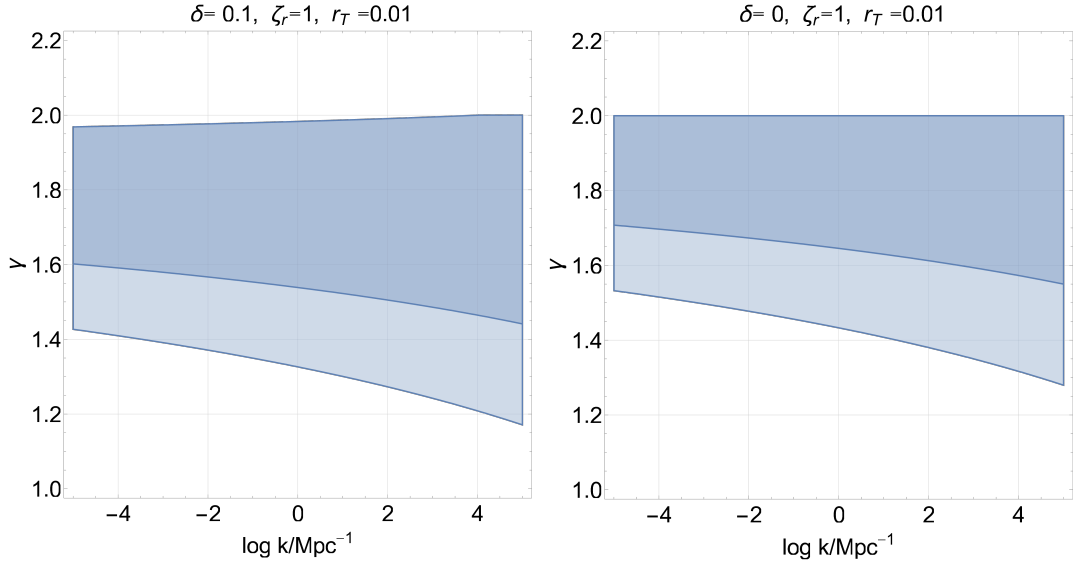


Figure 9: The allowed region of the parameter space is illustrated with a shaded area for fixed δ and in the (γ, k) plane. The different shading corresponds to the two extreme values of ξ appearing in Eq. (5.17).

were known also in Refs. [23] and suggested the idea that to have a successful magnetogenesis scenario we should necessarily consider a dynamical situation where, in the language of this paper, the gauge coupling decreases. Only in this case we could obtain a quasi-flat magnetic spectrum during the quasi-de Sitter phase. Even if it has been later on recognised that non only the inflaton but also some other spectator fields could effectively play the role of a dynamical gauge coupling [24] the conclusion remained: only if the gauge coupling decreases a flat hypermagnetic spectrum can be obtained during inflation.

The first observation is therefore that, within the present approach the twofold conclusion mentioned in the previous paragraph, follows directly from the dual treatment of the problem and of the related spectra; see, in particular the discussions after Eqs. (3.11)–(3.12) and also after Eqs. (3.26)–(3.27). For a number of years, it has been assumed that only when the gauge coupling decreases the magnetogenesis constraints could be satisfied [25]. This possibility has however some drawbacks that have been accurately discussed here (see subsections 2.4.1 and 2.4.2): if the hypermagnetic spectrum is flat during inflation strong coupling is expected when the gauge coupling starts its evolution.

The main idea of this paper has been to consider a more complete scenario where the gauge coupling first increases (or decreases) and then flattens out at late times as illustrated in Fig. 1 and 2. This approach, heavily based on the continuity of the mode functions and of the extrinsic curvature also considers specifically the transient regime where the gauge coupling relaxes and it does it in a computable manner. In the past the common approximation was that the gauge coupling (and hence $\sqrt{\lambda}$) abruptly freezes after inflation: we argued that this approach is not fully consistent a priori since it implies that the relevant pump fields (like $\sqrt{\lambda}''$) are singular across the inflationary boundary. If the gauge coupling flattens out in a smooth manner the present results showed that the late-time hypermagnetic power spectra outside the horizon in the radiation epoch are determined by the hyperelectric fields at the end of inflation whereas the opposite is true in the case of decreasing coupling. The obtained results then suggest that a slightly blue hyperelectric spectrum during inflation may lead to a quasi-flat hypermagnetic spectrum prior to matter radiation equality and before the relevant wavelengths reenter the effective horizon. Once more these results are a consequence of duality and of a very accurate analysis of the transition regime between the early inflationary stage and the subsequent evolution, as illustrated in Figs. 1 and 2. The obtained magnetic fields have been confronted with the magnetogenesis requirements and we can then conclude that large-scale magnetic fields can be generated during a quasi-de Sitter stage of expansion while the gauge

coupling remains perturbative throughout all the stages of the dynamical evolution.

The results of this analysis have been summarized in Figs. 9 and 10. In Fig. 9 the shaded areas denote the region where the spectral energy density is subcritical both during and after inflation while the magnetogenesis and the Cosmic Microwave Background (CMB) constraints are all satisfied. While the discussion of the CMB constraints would probably require a separate analysis, some general results could be used and these are essentially the ones reproduced in Fig. 6: they amount to requiring that the physical power spectrum after equality but before decoupling is smaller than 10^{-2} nG for typical wavenumbers comparable with the pivot scale $k_p = 0.002 \text{ Mpc}^{-1}$ at which the scalar and tensor power spectra are customarily assigned. The proper analysis of the CMB effects associated with the magnetic random fields started already after the first releases of the WMAP data; through the years various direct constraints have been derived both from the temperature and from the polarization anisotropies (see, for instance, [55] for a recent review). The main difference between the two plots of Fig. 9 stems from the magnetogenesis requirements: the larger area in the right plot corresponds to the situation where each galactic rotation amplifies the initial magnetic field value by one e -fold while the smaller area follows by requiring that the physical power spectrum exceed 10^{-22} nG^2 (see Eq. (5.17) and discussion therein). In Fig. 10 we consider the same constraints of Fig. 9 but in the (γ, δ) plane. The physical region obviously corresponds to the case $\delta \ll 1$.

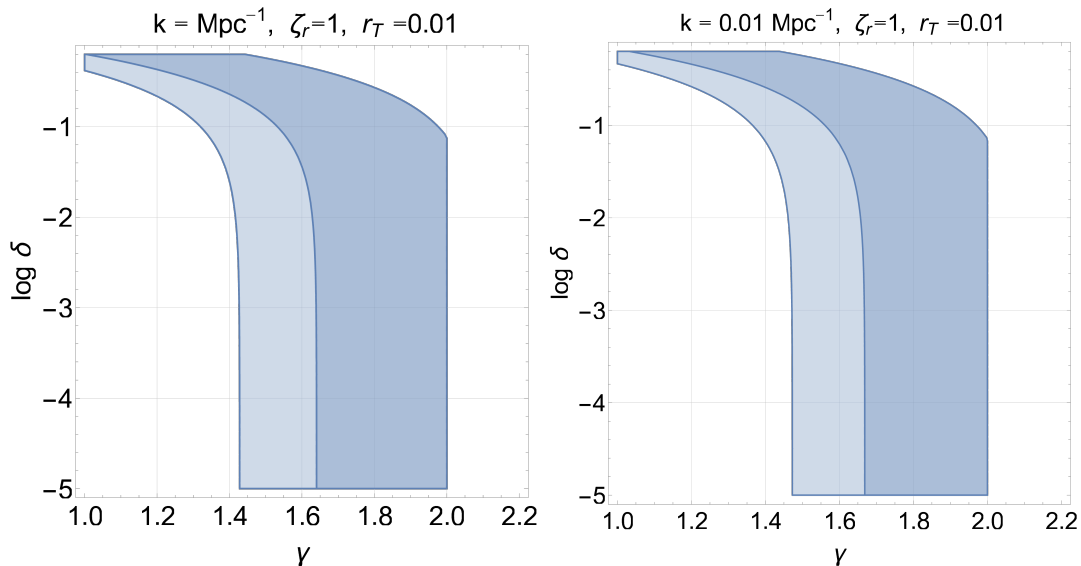


Figure 10: The allowed region of the parameter space is illustrated with a shaded area for fixed k and in the (γ, δ) plane. As in Fig. 9 the different shadings correspond to the two extreme values of ξ appearing in Eq. (5.17).

All in all we can conclude that magnetogenesis is phenomenologically viable in the perturbative regime provided the gauge coupling increases during a quasi-de Sitter stage and then flattens out after the end of the inflationary phase. The sweet spot of the parameter space (i.e. where all reasonable constraints are met) corresponds to a slightly increasing (blue) spectrum where $\mathcal{O}(1.6) \leq \gamma < 2$. If the magnetogenesis requirement are relaxed γ can be as small as $\mathcal{O}(1.4)$.

It does not make much sense to compare the present findings with the parameter space of the models where the gauge coupling decreases since, in those cases, a strongly coupled regime is expected at the onset of inflation. We instead conclude with a discussion of the various parameters of the scenario. These parameters are:

- γ and δ (or $\tilde{\gamma}$ and $\tilde{\delta}$ in the dual situation) describing the dynamics of the gauge coupling according to Figs. 1 and 2;

- the maximal inflationary scale which is however determined by the tensor to scalar ratio r_T which we took smaller than about 0.64 [50, 51];
- the possible presence of a post-inflationary phase whose length has been parametrized by ζ_r ;
- the expansion rate during the latter phase.

To these parameters we could eventually add $e_1 = \sqrt{4\pi/\lambda_1}$, i.e. the value of the gauge coupling at the end of inflation but this is implicitly included in the initial profile of the gauge couplings of Figs. 4 and 5. Depending on how we count we therefore have overall 5 or 6 parameters. If we would consider the case of instantaneous reheating the number of parameters could be reduced by 2. We are not interested here in the minimisation of the free parameters since the purpose of this paper is just to illustrate a potentially novel approach to the problem: more parameters might be included to account for more detailed physical aspects of the scenario. It is actually debatable if the minimisation of the parameters should be the ultimate purpose of a scenario and the sole criterion to assess its viability: an increase in the parameters typically entails a more accurate description of certain phenomena and a good example is actually the effect of reheating on magnetogenesis, as discussed above. Other examples could be made but it is not our purpose here to debate the heuristic value of this type of arguments.

6 Concluding considerations

Duality implies that the hypermagnetic power spectra parametrically amplified from quantum fluctuations during a quasi-de Sitter stage of expansion are scale-invariant (or slightly blue) if the gauge coupling decreases while an increase of the gauge coupling is only compatible with a flat hyperelectric spectrum for wavelengths larger than the effective horizon at the corresponding epoch. The same duality symmetry demands that the late-time gauge spectra do not always coincide with the results obtained at the end of inflation: the late-time hypermagnetic spectra follow directly from the hypermagnetic mode functions at the end of inflation whenever the gauge coupling decreases. Conversely if the gauge coupling increases the late-time hypermagnetic spectra are determined by the hyperelectric mode functions at the end of the inflationary phase. On a technical ground these results follow from the specific analysis of an appropriate transition matrix whose elements have well defined transformation properties under the duality symmetry and control the form of the late-time spectra.

Form a semiclassical viewpoint the mechanism analyzed here is the gauge analog of the Sakharov oscillations where travelling waves are transformed into standing waves with well defined phases that depend on the dynamics of the underlying geometry. The standing oscillations associated with the hyperelectric and with the hypermagnetic mode functions follow from the dynamics of the gauge couplings. Only when the gauge coupling decreases it is therefore reasonable to compute the post-inflationary physical spectra by a simple redshift of the comoving result during inflation. Conversely such a procedure would lead to an incorrect result in the case of an increasing gauge coupling where the late time hypermagnetic spectrum is determined by the hyperelectric spectrum at the end of inflation.

In summary, all the magnetogenesis constraints can be successfully satisfied when the gauge coupling remains perturbative throughout all the stages of its evolution. More precisely a slightly blue hyperelectric spectrum during inflation may lead to a quasi-flat hypermagnetic spectrum at late times. The induced large-scale magnetic fields turn out to be of the order of a few thousands of a nG over typical length scales between few Mpc and 100 Mpc. The magnetogenesis requirements are therefore satisfied together with all the backreaction constraints both during and after inflation. For the sweet spots of the parameter space the only further amplification required to seed the galactic magnetic fields is the one associated with the compressional amplification.

Acknowledgments

It is a pleasure to thank T. Basaglia and S. Rohr of the CERN Scientific Information Service for their kind help throughout various stages of this investigation.

A Transition matrix and increasing gauge coupling

In this first part of this appendix we shall consider a gauge coupling that sharply increases during the inflationary phase and then flattens out in the post-inflationary era. The profile of $\sqrt{\lambda}$ corresponds, in this case, to Eqs. (2.33)–(2.34) with $0 \leq \delta \ll \gamma$ (see also Fig. 1 and discussion therein). Since the parametrization of $\sqrt{\lambda}$ is continuous and differentiable the evolution of the mode functions during the post-inflationary stage (i.e. for $\tau \geq -\tau_1$) follows from the solution of Eqs. (2.20) and (2.21). For $\tau \geq -\tau_1$ the mode functions $f_k(\tau)$ and $g_k(\tau)$ are given in terms of certain coefficients $A_{\pm}(k, \tau_1)$:

$$f_k(\tau) = \frac{\sqrt{ky}}{\sqrt{2k}} \left[A_{-}(k, \tau_1) N_{\nu} H_{\nu}^{(1)}(ky) + A_{+}(k, \tau_1) N_{\nu}^{*} H_{\nu}^{(2)}(ky) \right], \quad (\text{A.1})$$

$$g_k(\tau) = \sqrt{\frac{k}{2}} \sqrt{ky} \left[A_{-}(k, \tau_1) N_{\nu} H_{\nu-1}^{(1)}(ky) + A_{+}(k, \tau_1) N_{\nu}^{*} H_{\nu-1}^{(2)}(ky) \right], \quad (\text{A.2})$$

where the following auxiliary quantities have been introduced:

$$\begin{aligned} N_{\nu} &= \sqrt{\frac{\pi}{2}} e^{i\pi(2\nu+1)/4}, & y(\tau) &= \tau + \tau_1(1+q), \\ q &= q(\delta, \gamma) = \frac{\delta}{\gamma}, & \nu &= \left(\delta + \frac{1}{2} \right). \end{aligned} \quad (\text{A.3})$$

The separate continuity of Eqs. (3.1)–(3.2) and (A.1)–(A.2) across $\tau = -\tau_1$, determines the explicit forms of $A_{\pm}(k, \tau_1)$ in the case²⁶ $\gamma > 1/2$:

$$\begin{aligned} A_{-}(k, \tau_1) &= \frac{i\pi N_{\mu}}{4N_{\nu}} \sqrt{q} x_1 \left[H_{\mu}^{(1)}(x_1) H_{\nu-1}^{(2)}(q x_1) - H_{\mu+1}^{(1)}(x_1) H_{\nu}^{(2)}(q x_1) \right], \\ A_{+}(k, \tau_1) &= \frac{i\pi N_{\mu}}{4N_{\nu}^{*}} \sqrt{q} x_1 \left[H_{\mu+1}^{(1)}(x_1) H_{\nu}^{(1)}(q x_1) - H_{\mu}^{(1)}(x_1) H_{\nu-1}^{(1)}(q x_1) \right], \end{aligned} \quad \gamma > 1/2, \quad (\text{A.4})$$

where $x_1 = k\tau_1$. For $0 < \gamma < 1/2$ the expressions of $A_{\pm}(k, \tau_1)$ are instead obtained by matching Eqs. (3.1) and (3.3) with Eqs. (A.1)–(A.2):

$$\begin{aligned} A_{-}(k, \tau_1) &= \frac{i\pi N_{\mu}}{4N_{\nu}} \sqrt{q} x_1 \left[H_{\mu}^{(1)}(x_1) H_{\nu-1}^{(2)}(q x_1) + H_{\mu-1}^{(1)}(x_1) H_{\nu}^{(2)}(q x_1) \right], \\ A_{+}(k, \tau_1) &= -\frac{i\pi N_{\mu}}{4N_{\nu}^{*}} \sqrt{q} x_1 \left[H_{\mu-1}^{(1)}(x_1) H_{\nu}^{(1)}(q x_1) + H_{\mu}^{(1)}(x_1) H_{\nu-1}^{(1)}(q x_1) \right], \end{aligned} \quad 0 < \gamma < 1/2. \quad (\text{A.5})$$

Since the electric and the magnetic mode functions must obey the Wronskian normalization of Eq. (2.21), $A_{\pm}(k, \tau_1)$ must satisfy the condition $|A_{+}(k, \tau_1)|^2 - |A_{-}(k, \tau_1)|^2 = 1$. If the mixing coefficients $A_{\pm}(k, \tau_1)$ are redefined as $\bar{A}_{+} = N_{\nu} A_{+}$ and $\bar{A}_{-} = N_{\nu}^{*} A_{-}$ the general expressions of Eqs. (A.1) and (A.2) become

$$f_k(\tau) = \frac{1}{\sqrt{2k}} \sqrt{ky} \left[\left(\bar{A}_{+} + \bar{A}_{-} \right) J_{\nu}(ky) + i \left(\bar{A}_{-} - \bar{A}_{+} \right) Y_{\nu}(ky) \right], \quad (\text{A.6})$$

$$g_k(\tau) = \sqrt{\frac{k}{2}} \sqrt{ky} \left[\left(\bar{A}_{+} + \bar{A}_{-} \right) J_{\nu-1}(ky) + i \left(\bar{A}_{-} - \bar{A}_{+} \right) Y_{\nu-1}(ky) \right]. \quad (\text{A.7})$$

Equations (A.6) and (A.7) can now be referred to the electric and magnetic mode functions of Eqs. (3.1) and (3.2)–(3.3) *evaluated at the end of inflation* i.e.

$$\begin{aligned} \bar{f}_k &= \frac{N_{\mu}}{\sqrt{2k}} \sqrt{x_1} H_{\mu}^{(1)}(x_1), & \bar{g}_k &= \sqrt{\frac{k}{2}} N_{\mu} \sqrt{x_1} H_{\mu+1}^{(1)}(x_1), & \gamma > 1/2, \\ \bar{f}_k &= \frac{N_{\mu}}{\sqrt{2k}} \sqrt{x_1} H_{\mu}^{(1)}(x_1), & \bar{g}_k &= -\sqrt{\frac{k}{2}} N_{\mu} \sqrt{x_1} H_{\mu-1}^{(1)}(x_1), & 0 < \gamma < 1/2, \end{aligned} \quad (\text{A.8})$$

²⁶The inflationary mode functions depend on the range of γ (see, in this respect, Eqs. (3.1) and (3.2)–(3.3)). Therefore that Eq. (A.4) only holds for $\gamma > 1/2$ while Eq. (A.5) holds for $0 < \gamma < 1/2$.

where, as in the bulk of the paper, $\bar{f}_k = f_k(-\tau_1)$ and $\bar{g}_k = g_k(-\tau_1)$. Since $x_1 = k\tau_1 < 1$ for all the modes of the spectrum the ratio of the mode functions of Eq. (A.8) can always be evaluated in the small argument limit and it is:

$$\left| \frac{k\bar{f}_k}{\bar{g}_k} \right| = \left| \frac{H_{|\gamma-1/2|}^{(1)}(x_1)}{H_{\gamma+1/2}^{(1)}(x_1)} \right| \rightarrow \frac{\Gamma(|\gamma-1/2|)}{\Gamma(\gamma+1/2)} \left(\frac{x_1}{2} \right)^{\gamma+1/2-|\gamma-1/2|}. \quad (\text{A.9})$$

The values of $f_k(\tau)$ and $g_k(\tau)$ for $\tau \geq -\tau_1$ will then be expressible in terms of \bar{f}_k and \bar{g}_k in the following manner

$$\begin{pmatrix} f_k(\tau) \\ g_k(\tau)/k \end{pmatrix} = \begin{pmatrix} A_{ff}(k, \tau, \tau_1) & A_{fg}(k, \tau, \tau_1) \\ A_{gf}(k, \tau, \tau_1) & A_{gg}(k, \tau, \tau_1) \end{pmatrix} \begin{pmatrix} \bar{f}_k \\ \bar{g}_k/k \end{pmatrix}. \quad (\text{A.10})$$

The entries of the matrix appearing at the right hand side of Eq. (A.10) have been given in Eq. (4.2); they follow directly from Eqs. (A.6)–(A.7) once the various coefficients are made explicit in terms of Eqs. (A.4) and (A.5).

B Transition matrix and decreasing gauge coupling

When the gauge coupling decreases Eqs. (2.41) and (2.42) describe the evolution of $\sqrt{\lambda}$ and of $\sqrt{\lambda}'$ interpolating between the inflationary stage and the subsequent radiation epoch (see also Fig. 2). In full analogy with Eqs. (A.1) and (A.2) the mode functions for $\tau \geq -\tau_1$ are determined in terms of a set of new coefficients $\tilde{A}_\pm(k, \tau_1)$:

$$f_k(\tau) = \frac{\sqrt{ky}}{\sqrt{2k}} \left[\tilde{A}_-(k, \tau_1) N_{\tilde{\nu}} H_{\tilde{\nu}}^{(1)}(ky) + \tilde{A}_+(k, \tau_1) N_{\tilde{\nu}}^* H_{\tilde{\nu}}^{(2)}(ky) \right], \quad (\text{B.1})$$

$$g_k(\tau) = -\sqrt{\frac{k}{2}} \sqrt{ky} \left[\tilde{A}_-(k, \tau_1) N_{\tilde{\nu}} H_{\tilde{\nu}+1}^{(1)}(ky) + \tilde{A}_+(k, \tau_1) N_{\tilde{\nu}}^* H_{\tilde{\nu}+1}^{(2)}(ky) \right], \quad \tilde{\delta} > \frac{1}{2}, \quad (\text{B.2})$$

$$g_k(\tau) = \sqrt{\frac{k}{2}} \sqrt{ky} \left[\tilde{A}_-(k, \tau_1) N_{\tilde{\nu}} H_{\tilde{\nu}-1}^{(1)}(ky) + \tilde{A}_+(k, \tau_1) N_{\tilde{\nu}}^* H_{\tilde{\nu}-1}^{(2)}(ky) \right], \quad 0 < \tilde{\delta} < 1/2, \quad (\text{B.3})$$

where, in analogy with Eq. (A.3), the following auxiliary quantities have been introduced:

$$\begin{aligned} N_{\tilde{\nu}} &= \sqrt{\frac{\pi}{2}} e^{i\pi(2\tilde{\nu}+1)/4}, & y(\tau) &= \tau + \tau_1(1+q), \\ q &= q(\tilde{\delta}, \tilde{\gamma}) = \frac{\tilde{\delta}}{\tilde{\gamma}}, & \tilde{\nu} &= \left| \tilde{\delta} - \frac{1}{2} \right|. \end{aligned} \quad (\text{B.4})$$

The expression of $\tilde{\nu}$ now depends on the range of $\tilde{\delta}$. More precisely for $\tilde{\delta} > 1/2$ the mixing coefficients are:

$$\begin{aligned} \tilde{A}_-(k, \tau_1) &= -\frac{i\pi N_{\tilde{\mu}}}{4N_{\tilde{\nu}}} \sqrt{qx_1} \left[H_{\tilde{\mu}}^{(1)}(x_1) H_{\tilde{\nu}+1}^{(2)}(qx_1) - H_{\tilde{\mu}-1}^{(1)}(x_1) H_{\tilde{\nu}}^{(2)}(qx_1) \right], \\ \tilde{A}_+(k, \tau_1) &= -\frac{i\pi N_{\tilde{\mu}}}{4N_{\tilde{\nu}}^*} \sqrt{qx_1} \left[H_{\tilde{\mu}-1}^{(1)}(x_1) H_{\tilde{\nu}}^{(1)}(qx_1) - H_{\tilde{\mu}}^{(1)}(x_1) H_{\tilde{\nu}+1}^{(1)}(qx_1) \right], \quad \tilde{\delta} > 1/2, \end{aligned} \quad (\text{B.5})$$

where, as in Eqs. (A.4)–(A.5), $x_1 = k\tau_1$. In the range $0 < \tilde{\delta} < 1/2$ we have instead that $\tilde{A}_\pm(k, \tau_1)$ are:

$$\begin{aligned} \tilde{A}_-(k, \tau_1) &= \frac{i\pi N_{\tilde{\mu}}}{4N_{\tilde{\nu}}} \sqrt{qx_1} \left[H_{\tilde{\mu}}^{(1)}(x_1) H_{\tilde{\nu}-1}^{(2)}(qx_1) + H_{\tilde{\mu}-1}^{(1)}(x_1) H_{\tilde{\nu}}^{(2)}(qx_1) \right], \\ \tilde{A}_+(k, \tau_1) &= -\frac{i\pi N_{\tilde{\mu}}}{4N_{\tilde{\nu}}^*} \sqrt{qx_1} \left[H_{\tilde{\mu}-1}^{(1)}(x_1) H_{\tilde{\nu}}^{(1)}(qx_1) + H_{\tilde{\mu}}^{(1)}(x_1) H_{\tilde{\nu}-1}^{(1)}(qx_1) \right], \quad 0 \leq \tilde{\delta} < 1/2. \end{aligned} \quad (\text{B.6})$$

As in the case of the results of appendix A, because of the Wronskian normalization of Eq. (2.21), the mixing coefficients of Eqs. (B.5)–(B.6) must satisfy $|\tilde{A}_+(k, \tau_1)|^2 - |\tilde{A}_-(k, \tau_1)|^2 = 1$. We can therefore summarize the situation by saying that while $A_\pm(k, \tau_1)$ of Eqs. (A.4)–(A.5) depend upon the range of γ , the $\tilde{A}_\pm(k, \tau_1)$ of Eqs. (B.5)–(B.6) depend on the range of $\tilde{\delta}$. Inserting the expressions of the coefficients (B.5) and (B.6) back into Eqs. (B.1), (B.2) and (B.3) the values of $f_k(\tau)$ and $g_k(\tau)$ for different values of $\tilde{\delta}$ can then be referred to the inflationary mode functions at $\tau = -\tau_1$ directly obtainable from Eqs. (3.22)–(3.23):

$$\bar{f}_k = \frac{N_{\tilde{\mu}}}{\sqrt{2k}} \sqrt{x_1} H_{\tilde{\mu}}^{(1)}(x_1), \quad \bar{g}_k = -N_{\tilde{\mu}} \sqrt{\frac{k}{2}} \sqrt{x_1} H_{\tilde{\mu}-1}^{(1)}(x_1), \quad (\text{B.7})$$

where $\tilde{\mu} = \tilde{\gamma} + 1/2$. As in the case of Eq. (A.9) the ratio of the mode functions of Eq. (B.7) can always be evaluated in the small argument limit and the result is:

$$\left| \frac{k \bar{f}_k}{\bar{g}_k} \right| = \left| \frac{H_{\tilde{\gamma}+1/2}^{(1)}(x_1)}{H_{|\tilde{\gamma}-1/2|}^{(1)}(x_1)} \right| \rightarrow \frac{\Gamma(\tilde{\gamma} + 1/2)}{\Gamma(|\tilde{\gamma} - 1/2|)} \left(\frac{x_1}{2} \right)^{|\tilde{\gamma}-1/2| - \tilde{\gamma}-1/2}. \quad (\text{B.8})$$

The magnetic and the electric mode functions for $\tau > -\tau_1$ can therefore be related to \bar{f}_k and \bar{g}_k of Eqs. (B.7) as:

$$\begin{pmatrix} f_k(\tau) \\ g_k(\tau)/k \end{pmatrix} = \begin{pmatrix} \tilde{A}_{ff}(k, \tau, \tau_1) & \tilde{A}_{fg}(k, \tau, \tau_1) \\ \tilde{A}_{gf}(k, \tau, \tau_1) & \tilde{A}_{gg}(k, \tau, \tau_1) \end{pmatrix} \begin{pmatrix} \bar{f}_k \\ \bar{g}_k/k \end{pmatrix}, \quad (\text{B.9})$$

where the explicit form of the various coefficients appearing at the right hand side of Eq. (B.9) has been reported in Eq. (4.29) which is the analog²⁷ of Eq. (4.2).

C Transition matrix and duality transformations

The transition matrices of Eqs. (A.10) and (4.29) are related by duality transformations. As it can be explicitly verified from Eqs. (2.33)–(2.34) and (2.41)–(2.42) a duality transformation implies that (γ, δ) are transformed into $(\tilde{\gamma}, \tilde{\delta})$:

$$\sqrt{\lambda} \rightarrow 1/\sqrt{\lambda} \quad \Rightarrow \quad \gamma \rightarrow \tilde{\gamma}, \quad \delta \rightarrow \tilde{\delta}. \quad (\text{C.1})$$

It has been shown [see Eq. (3.33) and discussion therein] that during inflation the transformation $\gamma \rightarrow \tilde{\gamma}$ exchanges electric into magnetic power spectra and vice versa. We shall now demonstrate that after inflation the corresponding duality transformation exchanges the elements of the transition matrices (A.10) and (4.29). Let us first start by noting that when $\delta \rightarrow \tilde{\delta}$ the corresponding Bessel indices ν and $\tilde{\nu}$ are related as:

$$\delta \rightarrow \tilde{\delta} \quad \Rightarrow \quad \nu \rightarrow 1 - \tilde{\nu}. \quad (\text{C.2})$$

Equation (C.2) is a consequence of the definitions of $\nu(\delta) = \delta + 1/2$ and $\tilde{\nu}(\tilde{\delta}) = |\tilde{\delta} - 1/2|$ given, respectively, in Eqs. (4.4) and (4.30). By now applying the transformation Eq. (C.2) to the matrix elements of $\mathcal{M}(\delta, x_1, x)$ and $\tilde{\mathcal{M}}(\tilde{\delta}, x_1, x)$ the following transformations are easily deduced:

$$A_{ff} \rightarrow \tilde{A}_{gg}, \quad A_{gg} \rightarrow \tilde{A}_{ff}, \quad (\text{C.3})$$

$$A_{fg} \rightarrow -\tilde{A}_{gf}, \quad A_{gf} \rightarrow -\tilde{A}_{fg}. \quad (\text{C.4})$$

²⁷Equations (4.29) and (4.2) do not coincide since ν and $\tilde{\nu}$ are different. Under duality, the elements of the transition matrices have a well defined transformation law given in Eq. (4.48) (see also appendix C hereunder). Along a similar perspective, unlike the case of Eqs. (3.2) and (3.3), the expression of $g_k(\tau)$ is unique for all the range of $\tilde{\gamma} > 0$; this occurrence follows from the difference between μ and $\tilde{\mu}$.

Equations (C.3) and (C.4) follow from the explicit expression of each matrix element. Consider, for instance, $A_{ff}(\delta, x_1, x)$ which we write, for immediate convenience, in terms of Hankel functions of first and second kinds:

$$A_{ff}(\delta, x_1, x) = \frac{i}{2} \sqrt{qx_1} \sqrt{ky} \left[H_{\nu}^{(1)}(ky) H_{\nu-1}^{(2)}(qx_1) - H_{\nu-1}^{(1)}(qx_1) H_{\nu}^{(2)}(ky) \right]. \quad (\text{C.5})$$

By now performing the transformation $\gamma \rightarrow \tilde{\gamma}$ and $\delta \rightarrow \tilde{\delta}$ (i.e. $\nu \rightarrow 1 - \tilde{\nu}$) we obtain, from Eq. (C.5),

$$A_{ff}(\tilde{\delta}, x_1, x) = \frac{i}{2} \sqrt{qx_1} \sqrt{ky} \left[H_{1-\tilde{\nu}}^{(1)}(ky) H_{-\tilde{\nu}}^{(2)}(qx_1) - H_{-\tilde{\nu}}^{(1)}(qx_1) H_{1-\tilde{\nu}}^{(2)}(ky) \right]. \quad (\text{C.6})$$

It is understood that while doing the transformation also the arguments of q and y will change according to Eqs. (4.4) and (4.30):

$$q(\delta, \gamma) = \delta/\gamma \rightarrow \tilde{\delta}/\tilde{\gamma} = q(\tilde{\delta}, \tilde{\gamma}), \quad (\text{C.7})$$

and similarly for y . We now recall that the Hankel functions of generic index μ and generic argument z obey [42, 43]

$$H_{-\mu}^{(1)}(z) = e^{i\pi\mu} H_{\mu}^{(1)}(z), \quad H_{-\mu}^{(2)}(z) = e^{-i\pi\mu} H_{\mu}^{(2)}(z). \quad (\text{C.8})$$

Inserting Eq. (C.8) into Eq. (C.6) we therefore obtain

$$A_{ff}(\tilde{\delta}, x_1, x) = -\frac{i}{2} \sqrt{qx_1} \sqrt{ky} \left[H_{\tilde{\nu}-1}^{(1)}(ky) H_{\tilde{\nu}}^{(2)}(qx_1) - H_{\tilde{\nu}}^{(1)}(qx_1) H_{\tilde{\nu}-1}^{(2)}(ky) \right], \quad (\text{C.9})$$

which coincides with $\widetilde{A}_{gg}(\tilde{\delta}, x_1, x)$, as anticipated in Eq. (C.3). With a similar procedure also the remaining transformation rules of Eqs. (C.3) and (C.4) can be easily deduced.

References

- [1] A. Lichnerowicz, *Magnetohydrodynamics: waves and shock waves in curved space-time*, (Kluwer academic publisher, Dordrecht, 1994).
- [2] S. Deser and C. Teitelboim, Phys. Rev. D **13**, 1592 (1976).
- [3] S. Deser, J. Phys. A **15**, 1053 (1982).
- [4] L. Parker, Phys. Rev. Lett. **21**, 562 (1968).
- [5] N. D. Birrell and P. C. W. Davies, *Quantum fields in curved space*, (Cambridge University Press, Cambridge, UK, 1982).
- [6] L. Parker and D. Toms, *Quantum Field Theory in Curved Spacetime: Quantized Fields and Gravity*, (Cambridge University Press, Cambridge, UK, 2009).
- [7] E. Fermi, Phys. Rev. **75**, 1169 (1949).
- [8] H. Alfvén, Phys. Rev. **75**, 1732 (1949); R. D. Richtmyer, E. Teller, Phys. Rev. **75**, 1729 (1949).
- [9] F. Hoyle, Proc. of Solvay Conference “*La structure et l’évolution de l’Univers*”, (ed. by R. Stoop, Brussels) p. 59 (1958).
- [10] Ya. B. Zeldovich, Sov. Phys. JETP **21**, 656 (1965) [Zh. Eksp. Teor. Fiz., **48** 986 (1965)].
- [11] K. S. Thorne, Astrophys. J. **148**, 51 (1967).
- [12] M. P. Ryan and L. C. Shepley *Homogeneous Relativistic Cosmologies* (Princeton, NJ, Princeton University Press, 1975).
- [13] E. R. Harrison, Phys. Rev. Lett. **18**, 1011 (1967).
- [14] E. R. Harrison, Phys. Rev. **167**, 1170 (1968).
- [15] M. Giovannini, Phys. Rev. D **62**, 123505 (2000).
- [16] H. Alfvén and C.-G. Fälthammer, *Cosmical Electrodynamics*, 2nd edn., (Clarendon press, Oxford, 1963).
- [17] E. N. Parker, *Cosmical Magnetic Fields* (Clarendon Press, Oxford, 1979).
- [18] Ya. B. Zeldovich, A. A. Ruzmaikin, D.D. Sokoloff *Magnetic Fields in Astrophysics* (Gordon Breach Science, New York, 1983).
- [19] K. Enqvist, Int. J. Mod. Phys. D **7**, 331 (1998).
- [20] M. Giovannini, Int. J. Mod. Phys. D **13**, 391 (2004); A. Kandus, K. Kunze, C. Tsagas, arXiv 1007.3891.
- [21] J. L. Han, Annu. Rev. Astron. Astrophys. **55**, 111 (2017).
- [22] S. Weinberg, “*Cosmology*”, (Oxford, Oxford University Press, 2008).
- [23] B. Ratra, Astrophys. J. Lett. **391**, L1 (1992); M. Gasperini, M. Giovannini, and G. Veneziano, Phys. Rev. Lett. **75**, 3796 (1995); M. Giovannini, Phys. Rev. D **64**, 061301 (2001).
- [24] K. Bamba and M. Sasaki, JCAP **02**, 030 (2007); K. Bamba JCAP **10**, 015 (2007); M. Giovannini, Phys. Lett. B **659**, 661 (2008).
- [25] K. Bamba, Phys. Rev. D **75** 083516 (2007); J. Martin and J. Yokoyama, JCAP **0801**, 025 (2008); M. Giovannini, Lect. Notes Phys. **737**, 863 (2008); V. Demozzi, V. Mukhanov and H. Rubinstein, JCAP **08**, 025 (2009).

- [26] I. Brown, *Astrophys. J.* **733**, 83 (2011); T. Fujita and S. Mukohyama, *JCAP* **1210**, 034 (2012); T. Kahniashvili, A. Brandenburg, L. Campanelli, B. Ratra and A. G. Tevzadze, *Phys. Rev. D* **86**, 103005 (2012); R. Z. Ferreira and J. Ganc, *JCAP* **1504**, 029 (2015); L. Campanelli, *Phys. Rev. D* **93**, 063501 (2016); C. Tsagas, arXiv 1412.4806; arXiv 1508.06604.
- [27] R. D. Peccei and H. R. Quinn, *Phys. Rev. Lett.* **38**, 1440 (1977); *Phys. Rev. D* **16**, 1791 (1977).
- [28] J. Kim, *Phys. Rep.* **150**, 1 (1987); H.-Y. Cheng, *ibid.*, **158**, 1 (1988); G. G. Raffelt, *Phys. Rep.* **198**, 1 (1990); *Lect. Notes Phys.* **741**, 51 (2008).
- [29] S. Carroll, G. Field and R. Jackiw, *Phys. Rev. D* **41**, 1231 (1990); W. D. Garretson, G. Field and S. Carroll, *Phys. Rev. D* **46**, 5346 (1992).
- [30] G. Field and S. Carroll *Phys. Rev. D* **62**, 103008 (2000); M. Giovannini, *Phys. Rev. D* **61**, 063502 (2000); *Phys. Rev. D* **61**, 063004 (2000); K. Bamba, *Phys. Rev. D* **74**, 123504 (2006); K. Bamba, C. Q. Geng and S. H. Ho, *Phys. Lett. B* **664**, 154 (2008).
- [31] L. Campanelli, *Int. J. Mod. Phys. D* **18**, 1395 (2009); L. Campanelli and M. Giannotti, *Phys. Rev. D* **72**, 123001 (2005); *Phys. Rev. Lett.* **96**, 161302 (2006); M. Giovannini, *Phys. Rev. D* **88**, 063536 (2013); K. Bamba, *Phys. Rev. D* **91**, 043509 (2015).
- [32] M. Giovannini and M. E. Shaposhnikov, *Phys. Rev. D* **57**, 2186 (1998); *Phys. Rev. Lett.* **80**, 22 (1998); M. Giovannini, *Phys. Rev. D* **61**, 063004 (2000).
- [33] M. Giovannini, *Phys. Rev. D* **61**, 063502 (2000); M. Dvornikov and V. B. Semikoz, *JCAP* **1202**, 040 (2012); S. Alexander, A. Marciano and D. Spergel, *JCAP* **1304**, 046 (2013); N. D. Barrie and A. Kobakhidze, *JHEP* **1409**, 163 (2014).
- [34] M. Giovannini, *Phys. Rev. D* **92**, 121301 (2015); *Phys. Rev. D* **93**, 103518 (2016).
- [35] D. E. Kharzeev, *Prog. Part. Nucl. Phys.* **75**, 133 (2014); M. Giovannini, *Phys. Rev. D* **88**, 063536 (2013).
- [36] D. Kharzeev, L. McLerran and H. Warringa, *Nucl. Phys. A* **803**, 227 (2008); K. Fukushima, D. Kharzeev and H. Warringa, *Phys. Rev. D* **78**, 074033 (2008); D. Kharzeev, *Annals Phys.* **325**, 205 (2010); M. Giovannini, *Phys. Rev. D* **94**, 081301 (2016).
- [37] A. D. Sakharov, *Sov. Phys. JETP* **22**, 241 (1966) [*Zh. Eksp. Teor. Fiz.* **49**, 345 (1965)].
- [38] P. J. E. Peebles and J. T. Yu, *Astrophys. J.* **162** 815 (1970).
- [39] R. A. Sunyaev and Y. B. Zeldovich, *Astrophys. Space Sci.* **7**, 3 (1970).
- [40] P. Naselsky and I. Novikov, *Astrophys. J.* **413**, 14 (1993).
- [41] S. Weinberg, *Phys. Rev. D* **67**, 123504 (2003).
- [42] A. Erdelyi, W. Magnus, F. Oberhettinger, and F. R. Tricomi *Higher Transcendental Functions* (Mc Graw-Hill, New York, 1953).
- [43] M. Abramowitz and I. A. Stegun, *Handbook of Mathematical Functions* (Dover, New York, 1972).
- [44] M. Giovannini, *J. Cosmol. Astropart. Phys.* **04** 003 (2010); *Phys. Rev. D* **85**, 101301 (2012).
- [45] M. Giovannini, *Class. Quant. Grav.* **26**, 045004 (2009); *Prog. Part. Nucl. Phys.* **112**, 103774 (2020).
- [46] A. Ito, J. Soda and M. Yamaguchi, [arXiv:2009.03611 [astro-ph.CO]].
- [47] K. Bamba, E. Elizalde, S. D. Odintsov and T. Paul, [arXiv:2012.12742 [gr-qc]].

- [48] T. Kobayashi and N. Afshordi, J. High Energy Phys. **10**, 166 (2014); C. Stahl, E. Strobel, and S. S. Xue, Phys. Rev. D **93**, 025004 (2016); R. Sharma and S. Singh, Phys. Rev. D **96**, 025012 (2017); E. Bavarsad, S. P. Kim, C. Stahl, and S. S. Xue, Phys. Rev. D **97**, 025017 (2018).
- [49] M. Giovannini, Phys. Rev. D **97**, 061301(R) (2018).
- [50] P. A. R. Ade *et al.* [BICEP2 and Keck Array Collaborations], Phys. Rev. Lett. **116**, 031302 (2016).
- [51] Y. Akrami *et al.* [Planck Collaboration], Astron. Astrophys. **641**, A10 (2020).
- [52] L. Kofman, A. D. Linde, and A. A. Starobinsky, Phys. Rev. Lett. **73**, 3195 (1994).
- [53] L. Kofman, A. D. Linde, and A. A. Starobinsky, Phys. Rev. D **56**, 3258 (1997).
- [54] L. Abbott, E. Farhi, and M. B. Wise, Physics Letters B **117**, 29 (1982).
- [55] M. Giovannini, Class. Quant. Grav. **35**, 084003 (2018).